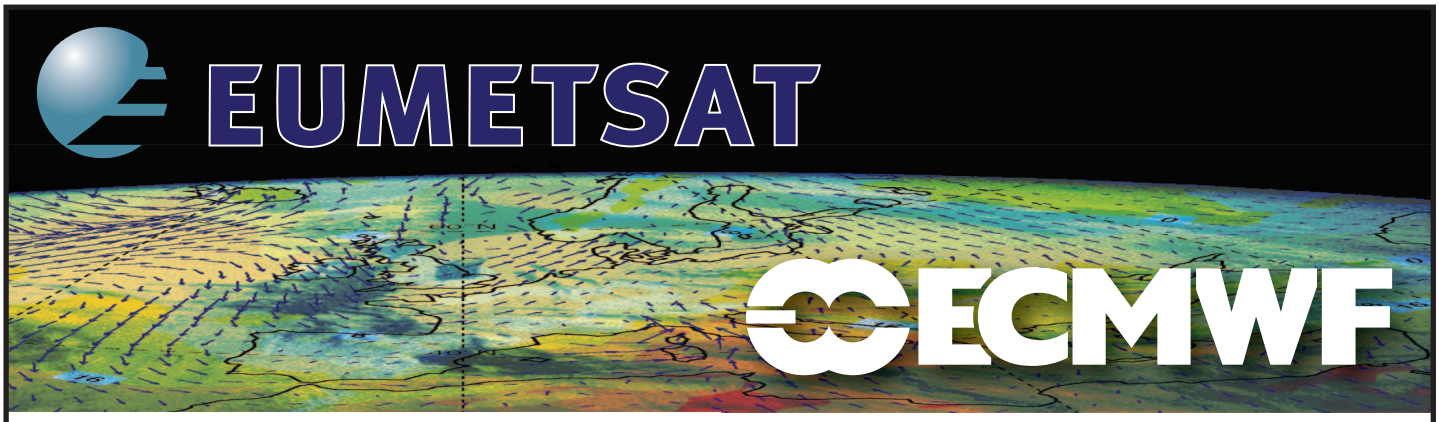


EUMETSAT/ECMWF Fellowship Programme
Research Report No. 25

# Assimilation of cloud-affected radiances from Meteosat-9 at ECMWF

Cristina Lupu and Anthony P. McNally

March 2012

Series: EUMETSAT/ECMWF Fellowship Programme Research Reports

A full list of ECMWF Publications can be found on our web site under:
http://www.ecmwf.int/publications/

Contact: library@ecmwf.int



European Centre for Medium Range Weather Forecasts
Shinfield Park, Reading, RG2 9AX, England

# 1 Executive summary

This past year, work has been directed towards incorporating all-sky radiances (ASR) from Meteosat-9 SEVIRI into the ECMWF four-dimensional variational assimilation (4D-Var) system, starting with the assimilation of cloud-affected radiances for restricted conditions such as overcast scenes. As dynamically active areas are known to be mainly cloudy, current aims in Numerical Weather Prediction (NWP) centers are to continue improvements in the assimilation of cloud-affected infrared radiances both in polar and geostationary orbits, with the idea that this is necessary for continuing gains in NWP skill.

At ECMWF cloud-affected infrared radiances in overcast conditions over the ocean from hyperspectral sounders (*i.e.*, Advanced Infrared Radiation Sounder and Infrared Atmospheric Sounding Interferometer) are already assimilated operationally. The model state vector is locally extended at observation locations, to include cloud top pressure and effective cloud fraction as cloud parameters. These parameters describing a single-layer cloud are simultaneously estimated together with temperature and humidity inside the main analysis. As part of this study, the ECMWF 4D-Var analysis system has been successfully extended to similarly assimilate cloud-affected geostationary radiances in overcast conditions from Meteosat-9. Initial 4D-Var assimilation experiments with overcast SEVIRI data as the only satellite data have lead to the following results:

- The assimilation of fully overcast infrared radiances was shown to systematically affect temperature, humidity and winds analysis increments in area of overcast cloud regimes, showing a very good correspondence between the altitude where the changes occur and the diagnosed height of the overcast cloud.
- The cloud parameters (i.e., cloud top pressure and effective cloud fraction) derived from SEVIRI ASR inside the 4D-Var agree well with independent EUMETSAT evaluation of the cloud conditions.
- Experimentation with the assimilation of cloud-affected SEVIRI radiances in the context of no-satellite baseline experiments have revealed the potential of overcast images for improving the wind tracing capability of SEVIRI radiances in 4D-Var.
- In general, low-level overcast scenes add most of the overcast situations to the system. Relaxing the overcast limitation by assimilating all scenes with an estimate effective cloud fraction greater than 0.99, leads to an increase of number of assimilated overcast scenes and better wind analysis scores. However, applying the simplified overcast approach to scenes with an estimate effective cloud fraction greater than 0.9 does not improve the wind analyses scores.

In the second part of this work a comparison has been made between the individual impact of each of the following observation types from Meteosat-9 SEVIRI: clear-sky radiances, overcast radiances and cloudy AMVs. The analysis impact of each observation type is expressed in terms of the root-mean-square of humidity and wind speed analysis difference with respect to a baseline assimilation. The main results of this comparison are:

- When the water-vapour clear-sky radiances are assimilated, the 4D-Var tracing mechanism fits the radiances by advecting deep layers of humidity and this leads to deeper layer adjustements of the wind field. For the cloudy AMVs the wind information is provided as a single level wind information and the structure functions of the background covariance matrix control the spread of this information on the vertical. SEVIRI AMVs data do not have significant impact on the relative humidity field. SEVIRI clear-sky radiances and cloudy AMVs impact is complementary with respect to the magnitude of wind increments and the altitude range at which each observation type has maximum impact.

- The vertical distribution of wind changes from assimilating cloud-affected radiances in overcast conditions and from cloudy AMVs are very similar in shape, showing a main peak at 250-300 hPa. The impact of AMVs is larger as the number of completely overcast SEVIRI scenes in the ASR product (48km x48km) is small compared to the number of cloudy AMVs.

The third phase of the study quantifyies the impact of the combined clear and overcast SEVIRI radiances on the wind analysis, compared with the impact of SEVIRI clear radiances alone and with the impact of cloudy SEVIRI atmospheric motion vectors (AMVs). The experiments show that:

- The extra cloudy radiances cover the areas where clear sky radiances are not available and provide useful additional temperature, humidity and winds increments in areas where they were assimilated.
- Wind speed vertical profiles from the combined clear and overcast radiances are rather similar in structure with those from just the clear SEVIRI data due mainly to the small volume of overcast data compared with the clear data. Larger impact at 300 hPa is obtained from the additional use of overcast scenes.
- Wind analysis scores show that combined clear and overcast SEVIRI radiances perform better than clear SEVIRI radiances alone particularly over the Southern Hemisphere. Over the Northern Hemisphere and Tropics, wind analysis scores for the both datasets are very close.

Finally, the potential operational benefits of assimilating overcast radiances from Meteosat-9 in addition to the clear radiances have been assessed in a full system where all routinely available observations are used. Results are clearly positive and the operational switch to ASR from Meteosat-9 in the next coming cycle (CY38R1) should improve the quality of 4D-Var analyses and subsequent forecasts. Work is well under way to assess the impact of all-sky SEVIRI observations in the assimilation and forecast system in terms of DFS diagnostics and forecast error contribution (FEC).

## 2 Introduction

A number of studies were conducted in recent years in NWP centres to investigate the capability to assimilate cloud-affected satellite data, with special focus on infrared observations obtained from hyperspectral sounders (Heilliette and Garand, 2007; Pavelin *et al.*, 2008; McNally, 2009; Pangaud *et al.*, 2009). These efforts aim on improving the sounder radiance data usage in cloudy regions that are meteorologically sensitive (McNally, 2002). The reader is referred to Bauer *et al.*, (2011) for details on the current development status of the assimilation of satellite observations affected by cloud in differents NWP centres. The ECMWF main impact of adding cloud-affected hyperspectral infrared observations is marginally positive on 500 hPa geopotential over the Northern and the Southern Hemispheres extratropics and positive on 700 hPa temperatureas at all latitudes (McNally, 2009).

Cloud-affected infrared radiances from geostationary satellites can also be beneficial to improve the forecast quality of NWP systems. There has been some progress recently in the assimilation of cloud-affected infrared brightness temperature from geostationary satellites.

The impact of cloud-affected satellite radiances from Meteosat-8 in the HIRLAM analysis and forecast accuracy had been evaluated by Stengel *et al.*, (2010). Following the approach proposed in Chevallier *et al.*, (2004) the observation operator was designed to diagnoses itself profiles of cloud cover and cloud condensate from the background values of the model state vector variables rather than using prescribed cloud top height and cloud cover. It was found that the assimilation of cloud-affected geostationary radiances improve the forecast accuracy

in the mid and upper troposphere. However, Stengel *et al.*, (2010) showed some degradation of the temperature and humidity forecast accuracy due to SEVIRI cloud-affected radiances at levels around 850 hPa in HIRLAM system.

The performance of a simple one-layer cloud scheme as described in McNally (2009), only constrained by cloud-top height and cloud fraction, has been recently investigated with simulates super-ob radiances of the MTSAT-1R imager in cloudy conditions (Okamoto, 2012). Data assimilation experiments with cloud-affected MTSAT-1R radiances in channel at 10.8 $\mu$m show a slightly improved forecast of temperature around 300 hPa and of winds in the lower troposphere.

In this paper, the feasibility of assimilating Meteosat-9 all-sky SEVIRI radiances directly into ECMWF 4D-Var is investigated. Following the approach described by McNally (2009), the performance of one-layer cloud-scheme constrained by cloud top height and cloud fraction has been investigated within an operational context with the all-sky radiances produced by EUMETSAT from SEVIRI.

Meteosat-9 is the prime observational satellite at $0^o$ longitude, in geostationary orbit, 35 800 km above the Gulf of Guinea, with a Spinning Enhanced Visible and InfraRed Imager (SEVIRI) on board. This optical imaging radiometer observes the Earth's atmosphere and surface in twelve channels: three in the visible (0.4-1.1, 0.6, 0.8 $\mu$m), one in the near-infrared (1.6 $\mu$m) and eight in the infrared (3.9 $\mu$m - 13.4 $\mu$m) and provide measurements with a resolution of 3 km by 3 km at the subsatellite point every 15 minutes (Schmetz *et al.*, 2002). Since 2004, infrared radiance data from SEVIRI were disseminated as a clear-sky radiance product. Along with the mean brightness temperatures for cloud free pixels in a 48 km by 48 km square box (i.e, 16 pixels by 16 pixels) the amount of the segment free of cloud expressed as percentage is also given with the EUMETSAT CSR product. The direct assimilation of Meteosat WV CSR data in the ECMWF 4D-Var system is discussed in detail in Munro *et al.* (2004) and Köpken *et al.* (2004). Since 2009, EUMETSAT started to disseminate the new ASR product generated hourly in a 16 pixels by 16 pixels square box (i.e, 48 km by 48 km at sub-satellite point). The ASR product contains brightness temperatures information from all water vapour and infrared channels averaged over all pixels within a processing segment as well as clear-and cloudy-sky brightness temperatures averaged over all clear and all cloudy pixels, respectively. Along with the averaged CSR and ASR, the percent of pixels flagged as clear and cloudy considering three types of layer clouds (high, middle and low) are also given by EUMETSAT.

Radiance measurements from geostationary infrared sensors from the WV channel provide valuable information on the mid- and upper tropospheric humidity field. Studies by Köpken *et al.* (2004), Munro *et al.* (2004) and Szyndel *et al.* (2005) have shown that the assimilation of high frequency CSR from geostationary satellites affects the 4D-Var wind field. Peubey and McNally (2009) have been clearly demonstrated that CSR leads to an improvement in ECMWF's 4D-Var wind analyses. They found that the most important mechanism through which the assimilation of CSR constrains the analysis is the humidity tracer advection which clearly dominate over the effects of balance constraints imposed on the analysis and model cycling. Clear-sky geostationary radiances have been found to improve the wind analysis throughout the troposphere, with the strongest signal in the middle and upper troposphere. It has also been shown that a single image at the end of a 12-hour assimilation window provides much larger impact than a single image at the beginning of it.

Currently, emphasis is being put on evaluating the extent to which useful information on humidity can be derived from cloud-affected SEVIRI radiances in ECMWF 4D-Var analysis. The main objective of this work was to extend the humidity tracing capability, previously demonstrated only in clear-sky to cloudy regions, to obtain an all-sky constraint on the atmospheric wind field with geostationary radiances. Of particular interest is the impact of the cloudy radiance data on the wind analysis via 4D-Var tracing, compared with cloudy AMVs. AMVs are useful for NWP because they provide wind observations with good coverage for the tropics and midlatitudes, especially over the large ocean areas.

Meteosat-9 atmospheric motion vectors datatsets are derived at EUMETSAT by tracking cloudy features in the infrared 10.8 $\mu$m channel, the 0.8 $\mu$m visible channel and from cloudy and clear-sky images in the 6.2 $\mu$m and 7.3 $\mu$m water vapour channels. The hourly Meteosat-9 AMVs disseminated by EUMETSAT is an average of three vectors calculated from a sequence of four images. Cloudy AMVs from Meteosat-9 are currently assimilated in the operational suite at ECMWF. Clear AMVs has not been used in this study because the height assignment is particularly problematic for clear-sky AMVs as the radiation in the WV channels under clear-sky conditions is emitted from a deep upper-tropospheric layer.

The structure of the paper is as follows. Section 3 describes an initial evaluation of overcast SEVIRI data in ECMWF 4D-Var. In Section 4, SEVIRI clear-sky radiances, overcast and cloudy AMVs observations have been introduced into a baseline (observation depleted assimilation system) in order to assess the impact on NWP wind analyses. Results from data assimilation experiments with overcast data assimilated in addition to the Meteosat-9 SEVIRI clear radiances are also discussed. Section 5 assesses the performance of SEVIRI ASR direct assimilation in low-resolution operation-like experiments. The impact of all-sky SEVIRI observations in the assimilation and forecast system is discussed in terms of DFS diagnostics and forecast error contribution. Finally, some conclusions are given in Section 6, while validation experiments using SEVIRI clear-sky radiances from both, CSR and ASR EUMETSAT products are described in Appendix I.

# 3 Assimilation of overcast SEVIRI radiance

The scheme used operationally at ECMWF to directly assimilate cloud-affected infrared radiances from polar orbiter data was extended to make use of the all-sky radiances from SEVIRI. The 4D-Var analysis control vector has been extended to include the cloud-top pressure $(C_P)$ and the effective cloud fraction $(C_F)$ as cloud parameters. In this approach clouds are assumed to be single-layer blackbody with a negligibile depth. The radiance observation operator RTTOV-9 (Matricardi *et al.*, 2004) is able to compute cloud-affected radiances using additional inputs of single-layer cloud-top height and fraction of opaque cloud. Background estimates of the additional analysis variables that describe clouds are diagnosed from the observations, not taken from the NWP model. Two channels per sensor, one around 13 $\mu$m and one around 11 $\mu$m (channels 6 and 8 for Meteosat-9) are used to define background estimates of cloud parameters and a value of 5 hPa has been used for the background error in cloud-top pressure. Following the approach introduced by Eyre and Menzel (1989) the estimation consists in minimizing the sum of the squared differences between observations and simulated cloudy radiances through the following cost function $J$:

$$J = \sum_{i=1}^{N} [R_{OBS} - R_{CLD}(C_P, C_F)]^2, \tag{1}$$

where $R_{OBS}$ is the observed radiance and $R_{CLD}$ is the cloudy radiance defined by a linear combination of overcast $R_O(C_P)$ and clear-sky radiances $R_{CLR}$ using the following equation:

$$R_{CLD}(C_P, C_F) = (1 - C_F)R_{CLR} + C_F R_O(C_P), \tag{2}$$

The first experiment uses an overcast SEVIRI observations addition onto a no-satellite baseline experiment over a one-month period from 10 February to 10 March 2010 (experiment identifier *fjvu,* hereafter exp_ov). The baseline has been initialized with the ECMWF operational analysis on 2 February 2010 and the only observations assimilated are conventional in situ data from radiosondes, aircraft and surface observations. Allowing the system to degrade over a period of 8 days, the base is then used as initial conditions for all the experiments performed in this study. Both assimilation experiments used 12-hour 4D-Var, with a model resolution of T511 corresponding to about 40 km, an incremental analysis resolution of T159 (125 km), and 91

levels in the vertical up to 0.01 hPa. If the scene was determined as overcast in the initial estimation process, the cloud fraction was fixed at 1.0 and four channels (6.2, 7.3, 10.8 and 13.4 $\mu$m) were activated in the analysis. Overcast scenes over land and ice surfaces or with an unreasonable cloud-top pressure or when the cloud top is determined to be below 900 hPa are not used in the current system. The observation errors assigned to each channel for overcast radiances have been kept to the same values (2K) as those for operationally assimilated clear-sky data. Additionally, the bias correction is the same for cloudy as well as clear conditions. Observational biases are corrected using variational bias correction, employing a linear bias model that includes a global constant, total column water vapour, 1000-300 hPa and 200-500 hPa layer thickness from the first-guess as predictors for WV channels and a global constant offset predictor for channels at 10.8 $\mu$m and 13.4 $\mu$m. In this experiment, VarBC coefficients were inherited from the previous cycle of the operational suite at T511 resolution (experiment identifier *fhha*) and they were updated at every analysis cycle.

Cloud fractions estimated within the ECMWF 4D-Var assimilation system from SEVIRI observations have been compared against independent estimates provided by EUMETSAT. Our estimation of effective cloud fraction, i.e., the product of fractional cloud cover and emissivity, agrees well with EUMETSAT independent estimation, especially for the overcast scenes (Lupu and McNally, 2011a).

Figure 1 displays the distribution of the overcast scenes from SEVIRI for the first assimilation window (00 UTC on 10 February 2010) separated into three categories depending on cloud height. The quality control decisions applied to overcast data leads to a rather low yield in terms of active observations available to the analysis. The overcast low clouds with the cloud top pressure between 600 and 900 hPa account for the majority of overcast scenes. An example of the coverage provided by the use of WV CSR from SEVIRI (channel at 6.2 $\mu$m) is also shown in Figure 1. It can be seen that the retained overcast data cover the areas where CSR are not available.

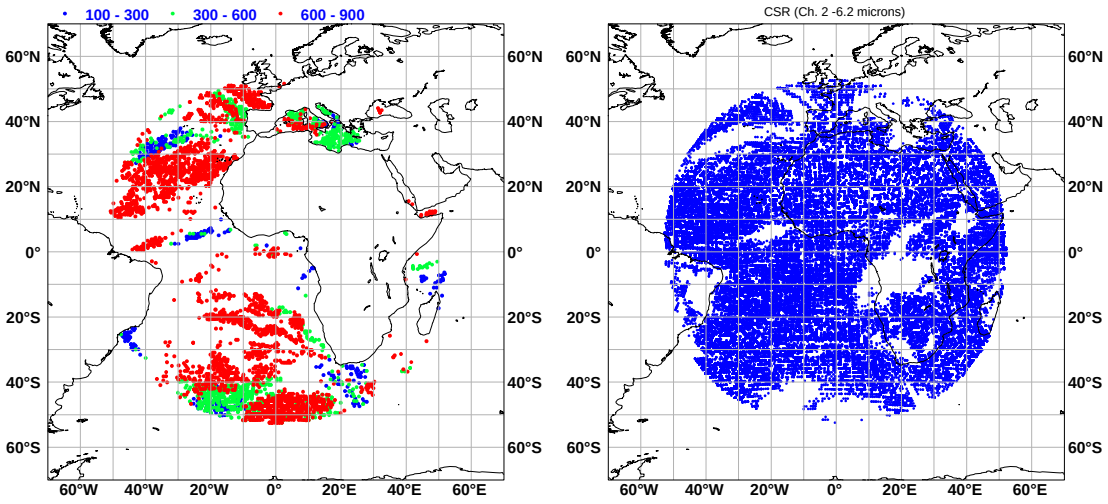


*Figure 1: The distribution of overcast cloudy scenes (left side) separated into three categories depending on cloud height (900-600 hPa (red), 600-300hPa (green), 300-100hPa (blue) and clear sky scenes (right side, blue dots) from SEVIRI water vapor channel at 6.2$\mu$m for the first 12-hour analysis cycle 00 UTC on 10 February 2010.*

The differences between temperature, humidity and wind analysis increments in the SEVIRI overcast experiment and the baseline has been examinated for the first 12-h analysis cycle. The increment differences at 300 hPa are shown in Figure 2 for temperature, humidity and winds. The assimilation of overcast SEVIRI radiances affects temperatures, humidity and winds in areas where overcast observations are assimilated showing a good correspondence between the altitude where the changes occur and the diagnosed height of the overcast cloud. After many successive cycles of assimilation the changes due to the use of overcast radiances spread by

advection into other areas.

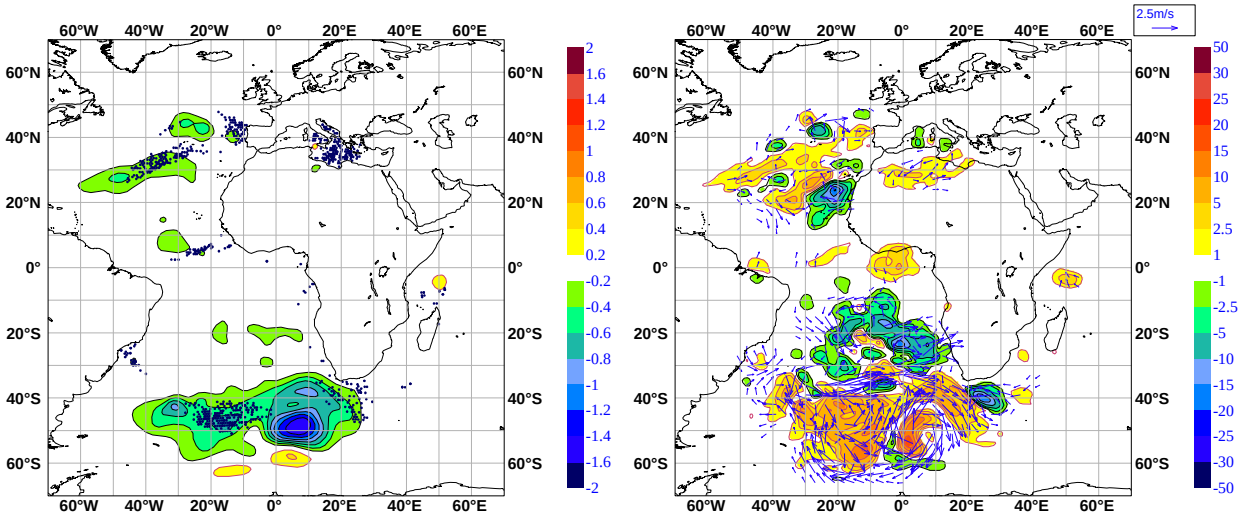


*Figure 2: For the first 12-hour analysis cycle (00 UTC on 10 February 2010), temperature increment differences (experiment minus baseline) (in K on the left), relative humidity (as a percentage) and winds (m/s, on the right side) produced by the overcast SEVIRI observations at 300 hPa (no-satellite context). The blue dots shows the location of overcast scenes with cloud height between 200-400 hPa.*

Overcast cloud-affected infrared radiance data from SEVIRI have been introduced into the ECMWF Integrated Forecasting System following the approach used operationally to directly assimilate cloud-affected radiance from advanced infrared sounders. This has permitted a comparison of cloud parameters calculated within the ECMWF 4D-Var assimilation system from SEVIRI observations with EUMETSAT independent estimates as well as an initial assessment of overcast SEVIRI data on ECMWF 4D-Var analysis. Overcast SEVIRI radiances have been shown to provide temperature, humidity and winds increments in area where the overcast observations were assimilated.

# 4 Baseline experiments : Wind tracing from SEVIRI clear and overcast radiance assimilation

The assimilation of high temporal density water vapour radiance data from geostationary satellites can influence the wind field through humidity tracer advection induced by 4D-Var. It has been demonstrated by Peubey and McNally (2009) that a 4D-Var assimilation system can derive useful tropospheric wind information from humidity sensitive radiances by advecting humidity features to improve the analysis fit to observations. In this section we investigate the impact of clear-sky radiances, overcast and cloudy AMVs observations from SEVIRI Meteosat-9 on 4D-Var wind analyses.

## 4.1 4D-Var humidity and wind increments from SEVIRI clear radiances, overcast radiances and cloudy AMVs

The results presented in this section were derived from experiments carried out with the ECMWF Integrated Forecasting System version CY36R3 at T511 resolution, 91 vertical levels and 12 hour 4D-Var for the period 10 February 2010 to 10 March 2010. SEVIRI radiances from the operational CSR product (experiment identifier

*Table 1: Summary of experiments performed in a no-satellite baseline context, discussed in Section 4.*

| Experiments | SEVIRI data used | | | Configuration |
|---|---|---|---|---|
| | Clear | OV | AMVs | Summary |
| *CSR* | yes | X | X | ch.2,3; Land/Sea; adapt. VarBC, more than 70% clear pixels. |
| *OV* | X | yes | X | ch.2, 3, 6, 8; Sea; adapt. VarBC; Cf=1. |
| *AMVs* | X | X | yes | IR, VIS0.8, cloudy WV6.2 and cloudy WV7.3 ; Land/Sea. |
| *OV1* | X | yes | X | ch.2, 3, 6, 8; Sea; static VarBC; Cf=1. |
| *OV2* | X | yes | X | ch.2, 3, 6, 8; Sea; static VarBC; Cf greater than 0.99. |
| *ex1_CLEAR* | yes | X | X | ch.2,3; Land/Sea; adapt. VarBC, more than 70% clear pixels. |
| *ex1_CLEAR+OV* | yes | X | X | CLEAR radiances: see ex1_CLEAR.<br>OV radiances: ch.2,3,6,8; Sea; adapt VarBC; high and medium overcast scenes with Cf=1. |
| *ex2_CLEAR* | yes | X | X | ch.2,3; Land/Sea; static VarBC, more than 70% clear pixels. |
| *ex2_CLEAR+OV* | yes | yes | X | CLEAR radiances: see ex2_CLEAR.<br>OV radiances: ch.2,3,6,8; Sea; static VarBC; Cf greater than 0.99 |

*fhg1*), overcast (OV) from ASR product (*fjvu*), cloudy AMVs SEVIRI observations (*firp*) as well as cloudy AMVs SEVIRI observations over oceans areas (*fk47*) were each added to a base experiment which uses a depleted observing system. The base (*fhfv*) has been initialized with the ECMWF operational analysis on 2 February 2010 and the only observations assimilated are conventional data from radiosondes, aircraft and surface observations. A summary of the main characteristics of the experiments ran to assess the wind analysis impact of SEVIRI observations is given in Table 1.

### *4.1.1 Impact of operational CSR and cloudy AMVs on analyses*

The procedure to assimilate the CSR and cloudy AMVs from SEVIRI in this study, is the same as in the current operational ECMWF suite.

In the CSR experiment, checks on brightness temperature and satellite zenith angles are applied and also a geographical thinning is performed prior to insertion into assimilation. CSR from WV channels are operational assimilated. SEVIRI data are assumed uncorrelated and a constant value of 2K has been assigned to the observation error standard deviation. For both WV channels, observational biases are corrected using variational bias correction, employing a linear bias model that includes a global constant, total column water vapour, 1000-300 hPa and 200-500 hPa layer thickness from the first-guess as predictors. SEVIRI CSR are thinned horizontally to $1.25^o$ and several quality control checks are applied. In the WV channel, all Meteosat-9 CSR having the percentage of clear pixels less than 70% are rejected and, over sea, data having background departure in the window channel outside a chosen range [-3K, 3K] are also excluded. In the window channel, CSR are passively monitored and used for quality control. In this channel, which have contributions from the surface, data over land and having a percentage of clear pixels less than 70% are blacklisted. In addition to the variational qualiy control checks a few data selection criteria are specified in the blacklist. For example, CSR observations having satellite zenith angles larger than $60^o$ or being over high terrain (higher than 1.5 km model orography) are excluded.

In the cloudy AMVs experiment, AMV data are horizontally thinned by selecting the AMVs with the highest

forecast independent quality indicator provided by EUMETSAT in boxes of 200 km by 200 km . AMVs are then assimilated hourly with observation errors of $2-6$ ms$^{-1}$.

To illustrate the wind tracing capability of geostationary SEVIRI radiances in 4D-Var, detailed comparisons with AMVs have been performed to study how the wind information from both data sources is distributed in the vertical (Lupu and McNally, 2011b). We display the analysis impact of each of SEVIRI CSR and cloudy AMVs in terms of the root-mean-square (RMS) of humidity and wind speed increment differences with respect to the Base assimilation in figure 3. These are shown as vertical profiles on pressure levels between 1000 hPa and 1 hPa for Meteosat-9 disc area.

In figure 3, the relative-humidity (left side) and wind impacts (right side), as provided by the RMS of the SEVIRI CSR experiment minus Base, is shown in blue line while the humidity and wind impact, as provided by the RMS of the SEVIRI AMVs experiment minus Base, is shown in black line. The vertical extent of the relative humidity increments, from WV CSR, typically between 100 and 800 hPa, and their peak, typically at 300 to 400 hPa, reflect the sensitivity of the WV channels. When the WV CSR are assimilated, the 4D-Var tracing mechanism fits the CSR by advecting deep layers of humidity and this leads to deeper layer adjustements of the wind field. For the cloudy AMVs the wind information is provided as a single level wind information and the structure functions of the background covariance matrix control the spread of this information on the vertical. However, SEVIRI AMVs data does not have significant impact on the relative humidity field. SEVIRI CSR and AMVs impact is complementary with respect to the magnitude of wind increments and the altitude range at which each observation type has maximum impact.

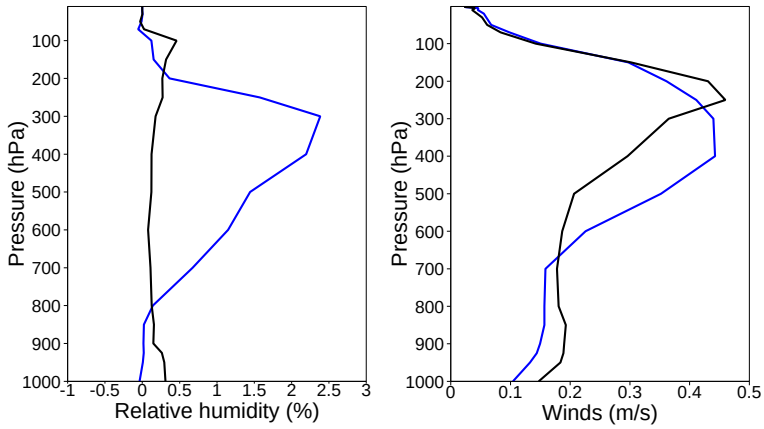


*Figure 3: Vertical profile of the monthly averaged RMS relative-humidity (left side) and wind speed (right side) increment differences between the CSR experiment minus base (blue line) and AMVs experiment minus base (black line).*

### *4.1.2 Impact of overcast and cloudy AMVs assimilated over sea on analyses*

Figure 4 displays the relative-humidity (left side) and wind impact (right side), as provided by the RMS of the SEVIRI OV experiment minus Base (blue line) and SEVIRI AMVs experiment minus Base (black line). As the overcast radiances (with an effective cloud fraction equal at 1) from four channels (6.2, 7.3, 10.8 and 13.4 microns) are only used over sea, the AMVs dataset is also used here over sea but not over land. Wind speed vertical profiles from overcast radiances and AMVs assimilated over sea, are very similar in shape, showing a main peak at 250-300 hPa. The impact of AMVs is larger as the number of completely overcast SEVIRI scenes is reduced comparatively with the number of cloudy AMVs. It appears that the humidity analysis increment difference is constrained to within 1.5% inside the Meteosat-9 disc in the Southern Hemisphere (latitude within

50°S-20°S) (not shown), where changes in monthly averaged humidity RMS increments above the cloud top are observed from the use of overcast data.

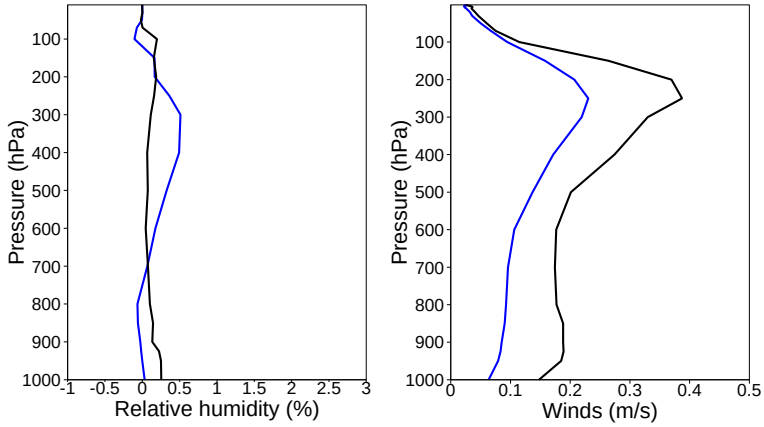


*Figure 4: Vertical profile of the monthly averaged RMS relative-humidity (left side) and wind speed (right side) increment differences between the overcast and base experiments (blue line) and AMVs over oceans and base experiments (black line).*

### *4.1.3 Wind analysis scores*

Peubey and McNally (2009) used the analysis scores to compare the wind analysis impact of CSR and AMVs derived from geostationary satellites. In this work a similar comparison has been performed for all experiments assimilating SEVIRI datasets: CSR, overcast, all cloudy AMVs and cloudy AMVs restricted to oceans areas. For each experiment, the wind analysis score is calculated inside Meteosat-9 disc by averaging over all $m$ assimilation cycles as follows:

$$\Delta\overline{RMSE} = \frac{\sum_{j=1}^{m}(RMSE_j^b - RMSE_j)}{\sum_{i=j}^{m} RMSE_j^b}. \tag{3}$$

where $RMSE_j$ and $RMSE_j^b$ are the wind analysis error for experiment and for the baseline, respectively. For every cycle $j$, wind analysis errors are calculated as departures from the ECMWF operational analysis that runs at T1279 resolution and assimilate the entire observing system as:

$$RMSE_j = \sqrt{\frac{1}{n}\sum_{i=1}^{n}(u_i - u_i^r)^2 + (v_i - v_i^r)^2}, \tag{4}$$

$$RMSE_j^b = \sqrt{\frac{1}{n}\sum_{i=1}^{n}(u_i^b - u_i^r)^2 + (v_i^b - v_i^r)^2}, \tag{5}$$

where $u_i$ and $v_i$ ($u_i^b$ and $v_i^b$) are the analysis values of the zonal and meridional wind components at a grid point $i$ for the experiment (baseline), $u_i^r$ and $v_i^r$ are the corresponding values from the ECMWF operations and $n$ is the number of grid points inside the considered area (longitude within 50°W-50°E, latitude within 20°N-50°N for the Northern Hemisphere, 20°S-20°N for the Tropics and 50°S-20°S for the Southern Hemisphere).

When a data set is added to the baseline the resulting analysis is always expected to perform better when compared to baseline. A zero value of the analysis score means no improvement over the baseline while the 100% value corresponds to an analysis that has no error with respect to the operational analysis.

Figure 6 shows the analysis scores of the wind speed for all experiments assimilating overcast, CSR and AMV SEVIRI data. Vertical error bars superimposed upon the plot indicate 95% confidence interval for wind analysis scores and were calculated using the Student distribution as in Peubey and McNally (2009). In the Tropics at 300 hPa, no improvement over the baseline is found when overcast data are assimilated and this is related to the limited number of overcast scenes assimilated. Additionally, CSR and AMVs impact is complementary with respect to the magnitude of wind increments and the altitude range at which each observation type has maximum impact. The analysis scores indicate a positive impact of overcast SEVIRI data through the troposphere over the Southern Hemisphere and at 500 hPa over the Tropics.

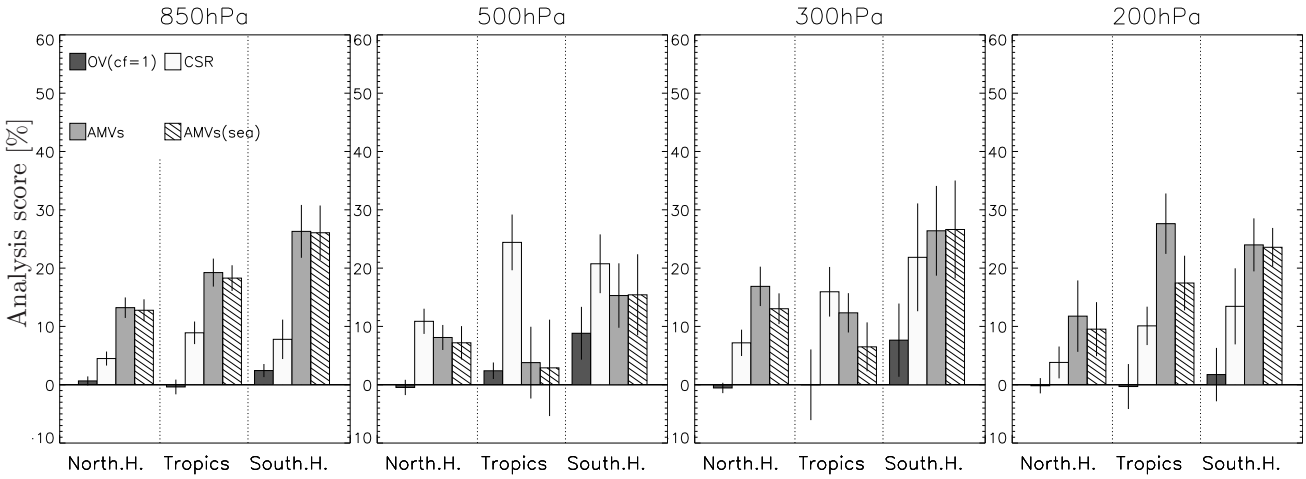


*Figure 5: Wind analysis scores calculated inside Meteosat-9 disc in the Northern Hemisphere [20°N-50°N], Tropics [20°S-20°N] and in the Southern Hemisphere [50°S-20°S] for the experiments assimilating SEVIRI overcast, CSR, cloudy AMVs and cloudy AMVs over oceans for one month assimilation period 10 February 2010 to 10 March 2010: OV (black), CSR(white), AMVs (dark grey) and cloudy AMVs over sea (hatched).*

## 4.2 Increasing the number of overcast SEVIRI data: impact on wind analyses

The evaluation of the daily evolution of the number of assimilated overcast observations in WV channels has shown that the number of active observations is not constant all along the study period. The number of assimilated observations drop by half in the first few assimilation cycles (figure 6, green line). Since we are interested here to maximize the number of assimilated overcast scenes, we examinated the impact of increasing the yield of overcast infrared data in the analysis. This was done first by applying a static bias correction scheme where the bias correction coefficients, first initialised with the corresponding VarBC coefficients from the operational suite, remain constant during all the experiment and second, by relaxing the restriction to strictly overcast data.

We summarize here the configurations of two additional experiments performed to increase the number of assimilated overcast observations: the first experiment (experiment identifier *fkgc* hereafter, exp_ov1) is identical to the previous one (only completely overcast scenes was assimilated) except that a static VarBC was used. In the second experiment (*fkgd* hereafter, exp_ov2), the strict limitation of using only completely overcast situations was relaxed by assimilating all scenes with effective cloud fraction greater than 0.99 and also, using a static VarBC. Using the static VarBC, the calculated bias parameters from the operational dataset are assumed to apply statically over time.

Figure 6 shows the number of daily assimilated overcast observations for water-vapour channel at 6.2 $\mu$m in the experimental overcast system and in the two additional experiments performed. Relaxing the overcast

limitation by assimilating all scenes with an estimate effective cloud fraction greater than 0.99, leads to an increase of number of overcast scenes assimilated and better wind analysis scores, particularly over the Southern Hemisphere (figure 7). It is worth noting that applying the simplified overcast approach to scenes with an estimate effective cloud fraction greater than 0.9 does not improve the wind analyses scores (not shown).

Results using a no-satellite baseline have revealed the potential of overcast images for improving the wind analysis in a 4D-Var context, particularly over the Southern Hemisphere through the troposphere.

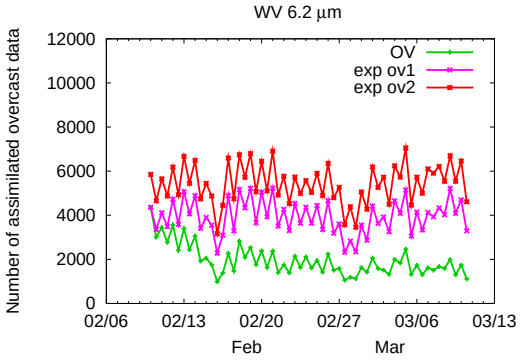


*Figure 6: Number of assimilated overcast SEVIRI in WV channel at 6.2 µm in the experimental overcast system OV (green line) and in two additionnal overcast : exp_ov1 (pink line) and exp_ov2 (red line).*

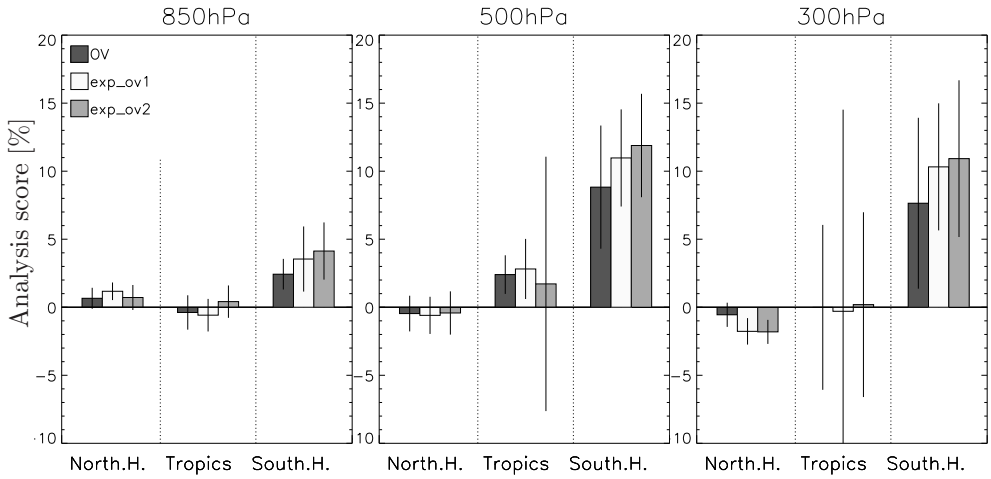


*Figure 7: Wind analysis scores calculated inside Meteosat-9 disc in the Northern Hemisphere [20°N-50°N], Tropics [20°S-20°N] and in the Southern Hemisphere [50°S-20°S] for three experiments assimilating SEVIRI overcast data for one month assimilation period 10 February 2010 to 10 March 2010: OV (black), exp_ov1(white), exp_ov2 (dark grey).*

## 4.3 4D-Var humidity and wind increments from SEVIRI clear radiances combined with overcast radiances

Using the new ASR products disseminated by EUMETSAT, the next step was to assimilate Meteosat-9 overcast data in addition to the clear radiances from the two water-vapour channels. In cloud free locations two WV channels from the ASR are used (6.2 and 7.3 microns, as was done for the previous CSR data), but for overcast scenes, four channels are assimilated (6.2, 7.3, 10.8 and 13.4 microns), the extra channels being required to determine the cloud conditions.

The ASR file contains brightness temperatures information from all water vapour and infrared channels averaged over all pixels within a processing segment ($T_B^{ALL}$) as well as clear- and cloudy-sky brightness temperatures averaged over all clear ($T_B^{CLR}$) and all cloudy pixels ($T_B^{CLD}$), respectively. An examination of the ASR BUFR file revealed that $T_B^{ALL} = T_B^{CLR}$ when the scene is completely clear (i.e., the percent of pixels flagged as clear-sky is 100%) and $T_B^{ALL} = T_B^{CLD}$ for completely overcast scenes (i.e., the percent of either high-, middle- or low-levels clouds or their sum is 100% and the percent of pixels flagged as clear-sky is 0%). Particularly, for WV channel at 6.2$\mu$m, a more detailed classification was found as follows:

- $T_B^{ALL} = T_B^{CLD}$ when the percent of either high-, mid-levels clouds or their sum is 100% and the percent of low-level clouds is 0% and the percent of pixels flagged as clear-sky is 0%.
- $T_B^{ALL} = T_B^{CLR} = T_B^{CLD}$ when the percent of low-level clouds is 100% and the percent of pixels flagged as clear-sky is 0%;

In the following, ASR were added to the same base experiment which use a depleted observing system (*fhfv*). Two potential configurations were evaluated for the assimilation of SEVIRI clear radiances combined with overcast radiances. Wind analysis score calculations are done for each configuration as well as for the pair experiment assimilating only the clear SEVIRI radiances.

The first configuration tested (hereafter, ex1_CLEAR+OV) was to use, in addition to the clear-sky brightness temperatures, the cloudy-sky brightness temperatures for all high and middle scenes identified by EUMETSAT as overcast. In this scenario, overcast radiances in four channels whose effective cloud fraction estimated as 1.0 was coincident with EUMETSAT high or middle overcast scenes with cloud top pressure ranges between 100 and 600 hPa were assimilated with the overcast approach (*fivg*). If the overcast scene fails to meet those requirements or if the scene is not overcast, the cloud fraction is fixed at zero and the system reverts to a clear-sky treatment of SEVIRI data. The adaptative variational bias correction was applied to both clear- and cloud-affected radiances. The overcast radiances are assimilated only over sea and the same quality control decisions as for the assimilation of clear radiances as in ex1_CLEAR+OV experiment was applied for a pair experiment assimilating only the clear radiances dataset (hereafter ex1_CLEAR, *fivf*).

Figure 8 shows the number of daily assimilated overcast observations in all four channes in the experimental cloudy system ex1_CLEAR+OV as well as the amount of clear SEVIRI radiances assimilated in both water-vapour channels in ex1_CLEAR and ex1_CLEAR+OV experiments. The additional overcast SEVIRI data assimilated in the ex1_CLEAR+OV experiment accounts for only 1.5% of the total of SEVIRI assimilated observations. The number of active clear SEVIRI observations is roughly the same in both experiments.

Figure 9 shows analysis scores of the wind speed calculated over the assimilation period 10 February 2010 to 10 March 2010 for the experiments assimilating SEVIRI clear radiances, SEVIRI clear radiances combined with overcast radiances restricted to high and middle overcast scenes and cloudy SEVIRI AMVs. In the context of no-satellite baseline experiment, SEVIRI clear radiances and SEVIRI clear radiances combined with overcast radiances have been found to improve the wind analysis throughout the troposphere. SEVIRI clear radiances combined with overcast radiances restricted to high and middle overcast scenes have a better performance than clear radiances dataset particularly over the Southern Hemisphere at 300 hPa.

The second configuration to possibly increase the number of overcast scenes in the assimilation was to use the cloud-affected dataset in the initial estimation of overcast situations and the clear-sky dataset for the assimilation of clear scenes. In this scenario, overcast radiances from those four channels whose effective cloud fraction was larger than 0.99 were assimilated. For all overcast scenes with an estimated effective cloud fraction greater than 0.99 and the cloud top pressure ranges between 100 and 900 hPa, four channels were activated in the analysis and assimilated only over sea. For all non overcast situations, the cloud fraction was then fixed to zero

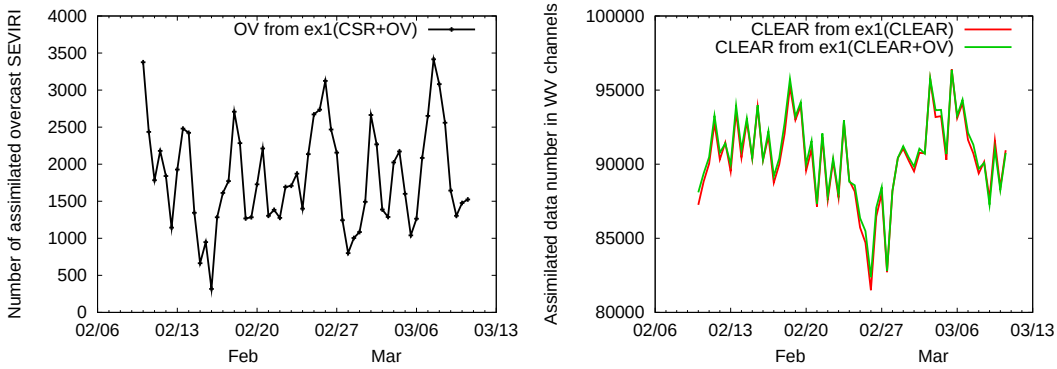


*Figure 8: Number of assimilated SEVIRI: (a) Overcast SEVIRI daily assimilated in four channels at 6.2 µm, 7.3 µm, 10.8 µm and 13.4 µm; (b) Clear SEVIRI data in both WV channels at 6.2 µm and 7.3 µm. The red line represents clear radiances from ex1_CLEAR experiment and the green line represents clear radiances from ex1_CLEAR+OV experiment.*

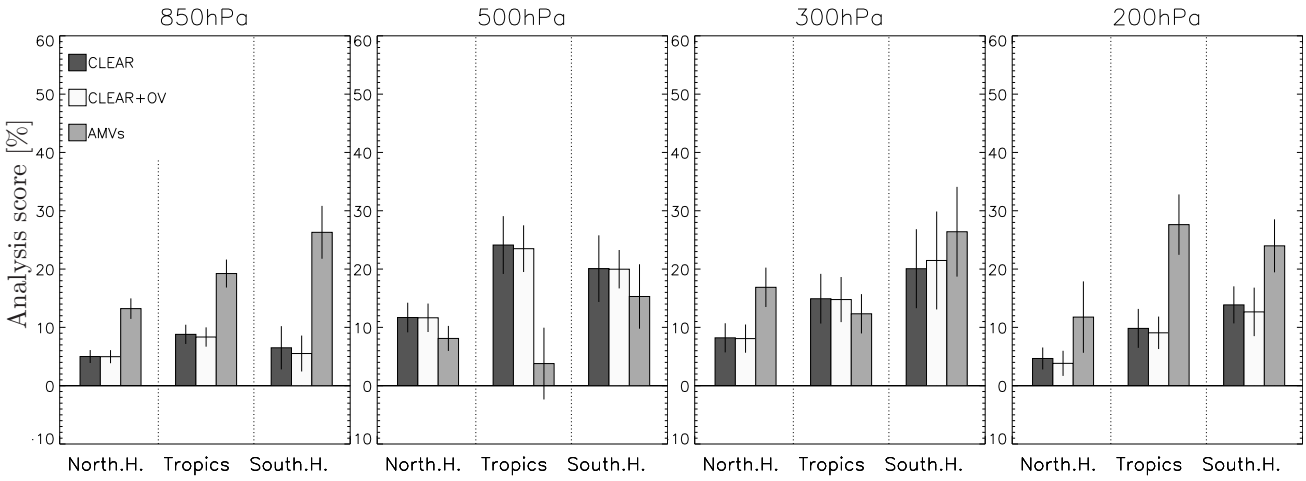


*Figure 9: Wind analysis scores calculated inside Meteosat-9 disc from 10 February 2010 to 10 March 2010 in the Northern Hemisphere [20°N-50°N], Tropics [20°S-20°N] and in the Southern Hemisphere [50°S-20°S] for the experiments assimilating SEVIRI clear radiances (ex1_CLEAR, black), SEVIRI clear radiances combined with overcast radiances restricted to high and middle overcast scenes (ex1_CLEAR+OV, white) and cloudy SEVIRI AMVs (dark grey).*

and the system will use the clear-sky brightness temperatures dataset for the direct assimilation of clear scenes. The assimilation of SEVIRI clear radiances in the combined ex2_CLEAR+OV (*flhc*) and ex2_CLEAR (*flh3*) experiments used the same data selection criteria. In both experiments a static VarBC was applied to both clear and overcast radiances. Using this configuration the number of daily assimilated overcast observations increase in the experiment ex2_CLEAR+OV (*flhc*) as shown in figure 10.

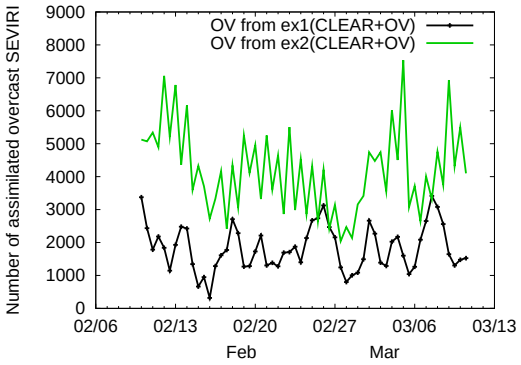


*Figure 10: Time series of the number of overcast SEVIRI daily assimilated in four channels in ex2_CLEAR+OV (experiment flhc, grey line) and ex1_CLEAR+OV (experiment fivg black line).*

An example of the additional coverage provided by the use of overcast data in the ex2_CLEAR+OV(*flhc*) is shown in figure 11 for the first 12-h assimilation window.

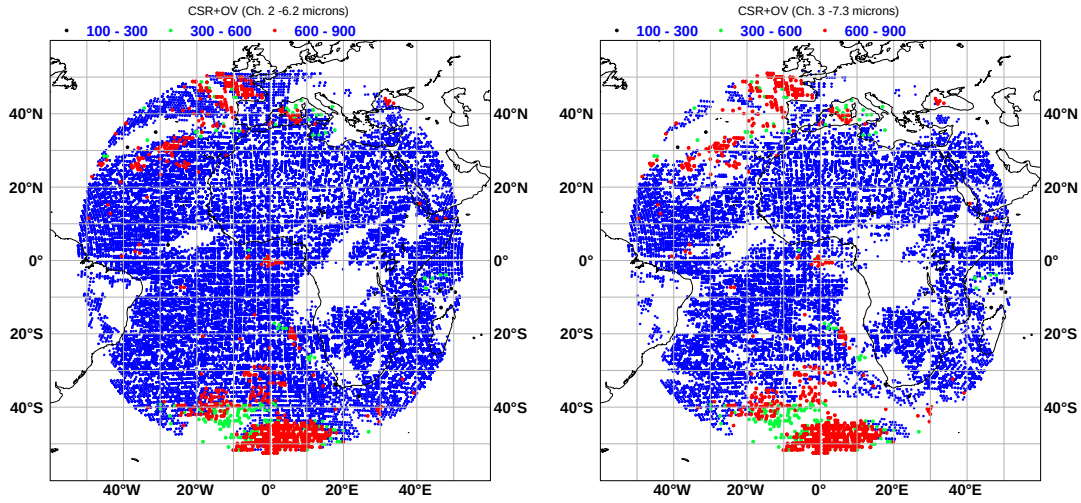


*Figure 11: The distribution of overcast cloudy scenes separated into three categories depending on cloud height (900-600 hPa (red), 600-300hPa (green), 300-100hPa (blue) and clear sky scenes (blue dots) from SEVIRI water vapor channels at 6.2µm (left side) and 7.3µm (right side) for the first 12-hour analysis cycle 00 UTC on 10 February 2010.*

The additional impact of the overcast SEVIRI radiances upon the assimilation system is illustrated in figure 12 as provided by the vertical profiles of RMS relative-humidity and wind speed increment differences from each of the ex2_CLEAR+OV, ex2_CLEAR and cloudy AMVs experiments and the base experiment. These have been estimated by substracting the humidity or wind speed increment of baseline experiment from the increment of the considered experiments. Wind speed increments from SEVIRI clear radiances (ex2_CLEAR) and SEVIRI clear radiances combined with overcast radiance (ex2_CLEAR+OV) are very similar in structure but a larger magnitude with a maximum at 300 hPa is obtained from the ex2_CLEAR+OV experiment particularly in the

Southern Hemisphere region inside of the Meteosat-9 disc. This demonstrate the effect of humidity-tracer advection involved in the production of wind increments from the additional assimilated overcast SEVIRI observations.

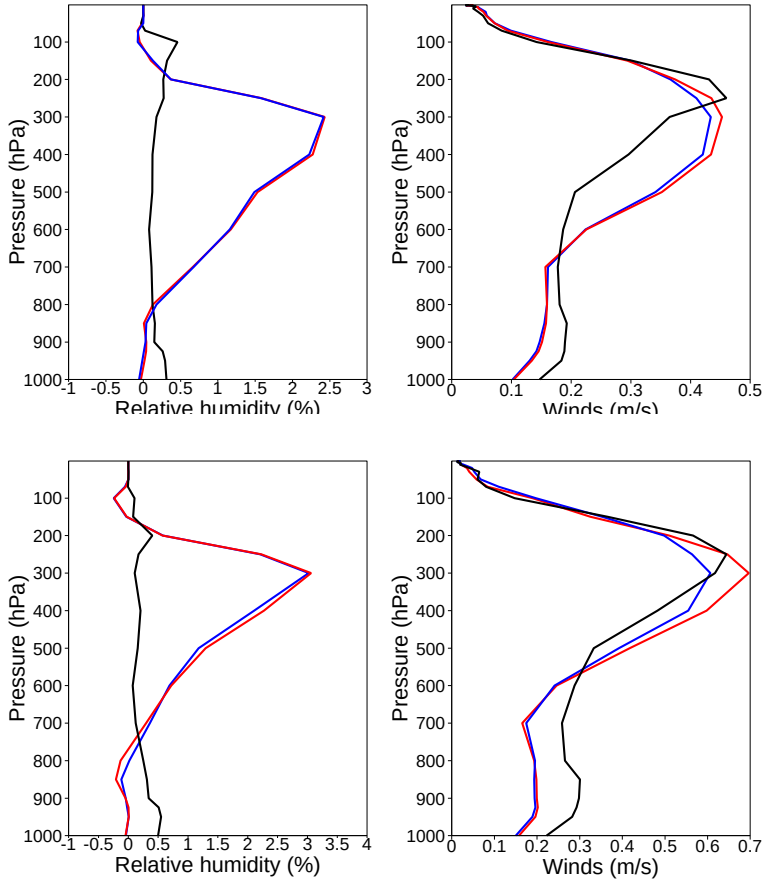


*Figure 12: Vertical profile of the monthly averaged RMS humidity and wind speed increment differences between: ex2_CLEAR+OV and base experiment (red line), ex2_CLEAR and base (blue line) and cloudy AMVs and base (black line) inside Meteosat-9 disc (top) and Southern Hemisphere (50°S-20°S, bottom)*

Analysis scores have been also calculated for the experiments described above and compared with cloudy AMVs results (fig. 13). In the context of no-satellite baseline experiment, ex2_CLEAR+OV have a positive impact on wind analyses through the upper-troposphere with better performance than ex2_CLEAR particularly over the Southern Hemisphere. Over the Northern Hemisphere and Tropics, wind analysis scores for the ex2_CLEAR+OV (white bars) and ex2_CLEAR (dark bars) are very close, showing that in those regions, wind analyses only get benefits from the clear radiance assimilation. However, over those regions the number of overcast scenes is limited. The impact of cloudy AMVs is significantly larger at 850 hPa and 200 hPa, owing to the large number of cloudy AMVs assimilated.

The results reported here are sufficiently encouraging in suggesting the potential benefits of assimilating overcast SEVIRI observations in wind analyses scores and justify further work. However, it should be noticed that in the context of a no-satellite baseline experiment, analysis errors are larger than might be expected from a full observing system. Consequently, the improvement in wind analysis scores from the combined clear and overcast dataset with respect to the clear dataset may be larger than would be expected when those data sets are added to a full observing system.

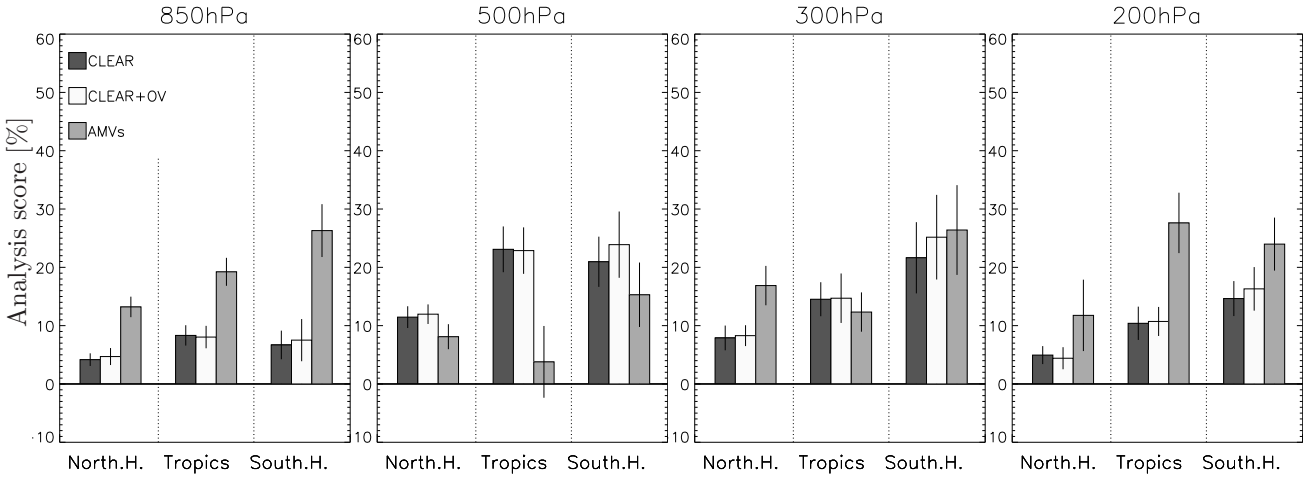


*Figure 13: Wind analysis scores calculated inside Meteosat-9 disc in the Northern Hemisphere [20°N-50°N], Tropics [20°S-20°N] and in the Southern Hemisphere [50°S-20°S] for the experiments assimilating SEVIRI clear, combined clear and overcast and cloudy AMVs for the assimilation period (10 February 2010 to 10 March 2010): CLEAR(black, ex2_CLEAR), CLEAR+OV (white, ex2_CLEAR+OV), AMVs (dark grey).*

The next section explores how the full operational forecasting system will work with EUMETSAT cloud-affected SEVIRI radiances.

# 5 Towards an operational assimilation of SEVIRI clear and overcast observations

Because a new cycle (CY37R3) went operational on 15th November 2011 at ECMWF, the modifications related to the assimilation of ASR products from Meteosat-9 were tested within this new cycle with the full observing system. Before looking to the additional use of overcast data, we had to validate SEVIRI clear dataset obtained from the new ASR product.

Experiments have been run in the global 4D-Var configuration with 12-hour assimilation window for winter period (1 January 2011 - 1 March 2011) and were based on a lower than operational horizontal resolution (T511 rather than T1279) to save computer resources. Initial conditions came from the operational analyses for 12Z on 31st December 2010. Only one medium-range forecast has been run per day as opposed to two forecasts in the operational configuration. The experiments carried out were therefore:

- Control experiment CTRL (*fkvl*) used all available conventional and satellite data, including WV Meteosat-9 clear-sky radiances from EUMETSAT CSR product.
- Experiment EXP1 (*fmr0*) is identical with the control experiment except that WV clear SEVIRI radiances from the new ASR product are assimilated in the place of SEVIRI WV CSR.
- Experiment EXP2 (*fms1*) has been designed to test the cloudy assimilation scheme with SEVIRI ASR. The experiment EXP2 uses the same selection criteria for the assimilation of WV clear SEVIRI radiances as the previous experiment EXP1 and exclude all scenes identified as overcast in the cloud parameters estimation process. The purpose of this experiment was to technically check the cloudy assimilation approach code changes and to validate that the performance of the assimilation system remain unchanged when only the clear SEVIRI dataset is assimilated.

Results of the validation experiments EXP1 and EXP2 using Meteosat-9 ASR were compared to the CTRL and were shown in the Appendix 1. The next section focus on the bias correction of SEVIRI data in 13.4 $\mu$m channel.

## 5.1 ECMWF bias monitoring statistics of SEVIRI data

An important part of assimilating satellite radiances such as SEVIRI is the bias correction since the differences between observed radiances and the model derived radiances are neither bias-free. In the control experiment, a bias correction is only calculated for the two assimilated WV channels and for the 10.8 $\mu$m channel (which is only corrected for its use in the observation quality control but is not directly assimilated). An examination of the equivalent statistics obtained over two months from Meteosat-9 in both experiments EXP2 and CTRL show almost identical results. An example is shown in Figure 14 that compares the time series of first guess and analysis departures for SEVIRI clear radiances in WV channels at 6.2 $\mu$m and 7.3 $\mu$m in the Northern Hemisphere. Identical biases are evident and VarBC is applying the same bias correction for clear Meteosat-9 radiances in both experiments. Similar findings are valid also for statistics over the Southern Hemisphere and Tropics and also for 10.8 $\mu$m channel (not shown).

In the EXP2, the 13.4 $\mu$m channel, used to estimate the cloud parameters, should be also bias corrected. A constant offset predictor was used to correct the differences between observed and model derived radiances. Due to the spectral location, its radiance shows temperature sensitivity through the troposphere with a maximum amplitude in the lower troposphere around 850 hPa. The 13.4 $\mu$m channel is also predicted to be most sensitive to ice contamination. Figure 15 shows the time series of first guess and analysis departures for clear SEVIRI observations from EXP2 in channel at 13.4 $\mu$m before and after bias correction. The amplitude of the signal in the uncorrected radiance departures that was nearly 2.16 K, is centered around 0.03 K after the VarBC scheme was applied.

The final aim of this study is to evaluate the impact of clear and overcast SEVIRI data from the ASR product with respect to the operational CSR dataset. Since in the ECMWF operational context clear-sky SEVIRI radiances from 10.8 $\mu$m and 13.4$\mu$m channels are not assimilated, in the next section further experimentation has been conducted only with SEVIRI clear and overcast radiances from WV channels at 6.2 $\mu$m and 7.3 $\mu$m.

## 5.2 Impact of SEVIRI ASR in the operational ECMWF system

Results of one assimilation experiment ASR (experiment identifier *fnf2*) run over the period 1 January 2011 - 31 March 2011 making additional use of overcast SEVIRI data over sea with an effective cloud fraction greater than 0.99 only in WV channels at 6.2 $\mu$m and 7.3 $\mu$m are now presented.

### *5.2.1 Analysis impact*

Departure statistics for the observing system are computed over the experiment period (from 1 January 2011 - 31 March 2011): mean and standard deviation of the differences between observations and NWP first guess are computed after the bias correction of satellite radiances. Over the Southen Hemisphere, the assimilation of combined SEVIRI clear and overcast radiances slightly improves the standard deviation of background and analysis departures in WV channel at 6.2 $\mu$m (e.g. Fig. 16). The fit to other assimilated observations are not changed in the ASR experiment compared to the CTRL (not shown), suggesting that both experiments agree similarly well with the rest of the observing network. Changes to the mean analyses are also very small for the troposphere.

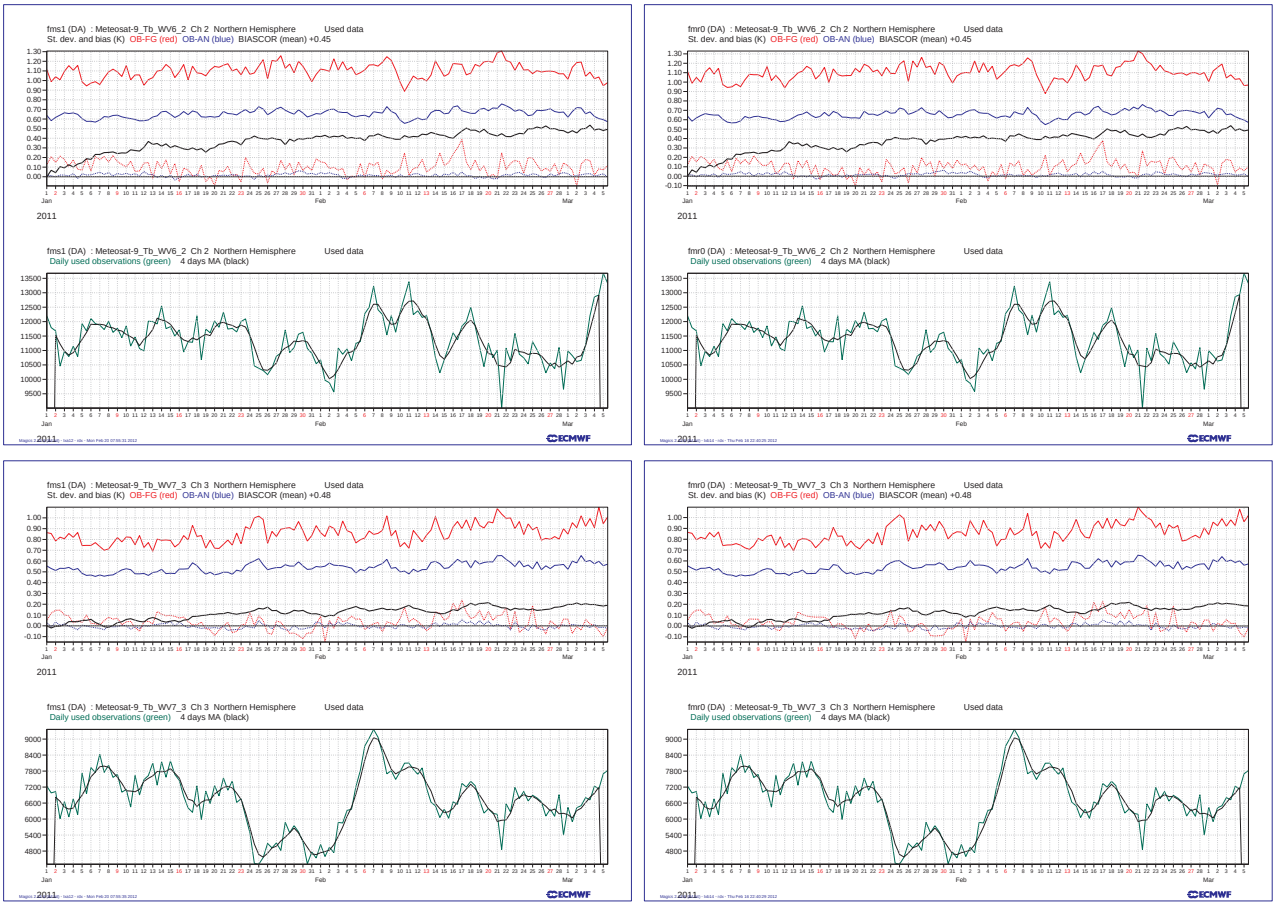


*Figure 14: Time series of mean and standard deviations of the first guess and analysis departures (before and after the bias correction) from EXP2 (left) and EXP1 (right) for CSR from SEVIRI in WV channel at 6.2 µm (top) and 7.3 µm (bottom) in the Northern Hemisphere. Also shown are the time series of bias correction and observation numbers.*

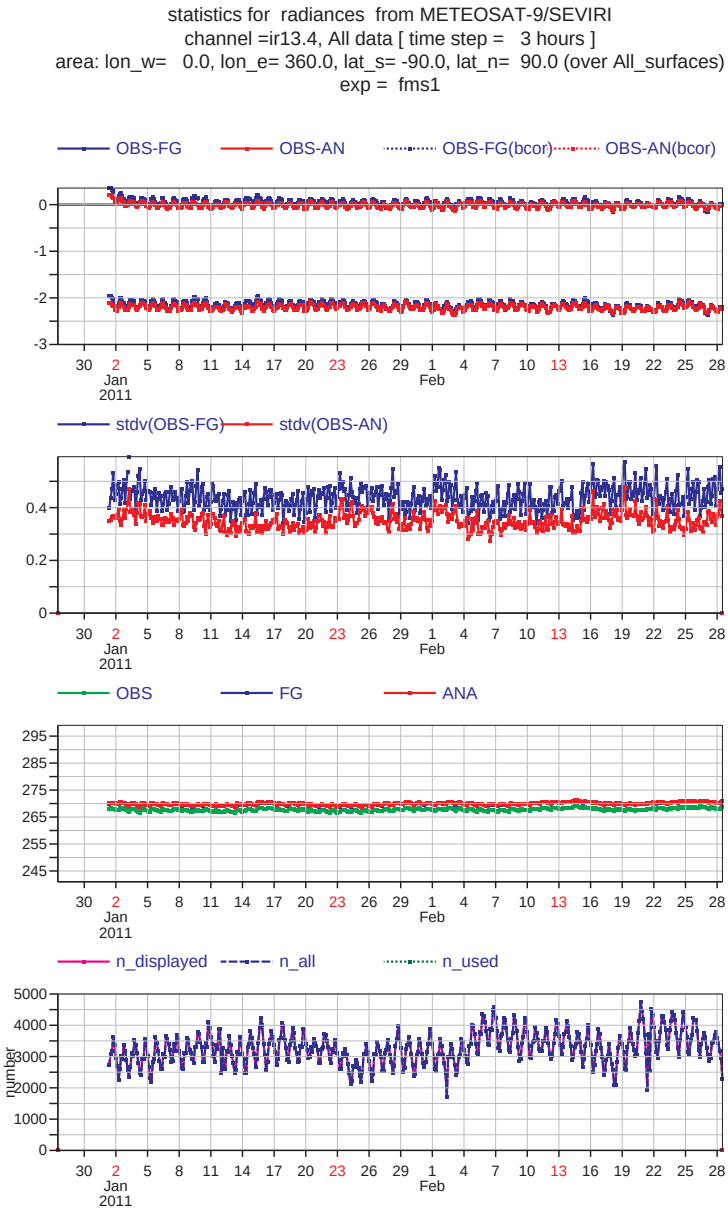


*Figure 15: Time series of mean and standard deviations of the first guess and analysis departures (before and after the bias correction) in EXP2 for all clear SEVIRI radiances in IR channel at 13.4 µm. Also shown are the time series of observation numbers.*

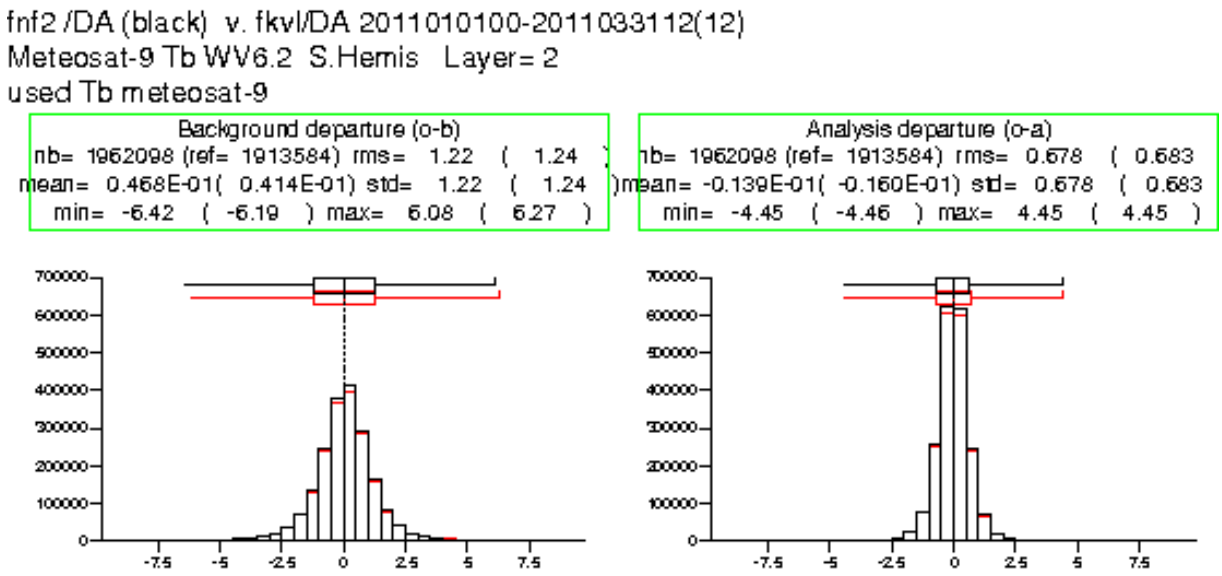


*Figure 16: Standard deviation and mean of the first-guess and analysis departures calculated over the Southern Hemisphere for SEVIRI water-vapour channel(6.2 µm) from ASR (black) and CTRL (red) experiments.*

### *5.2.2 Forecast impact*

To verify how atmospheric variables are affected by the Meteosat-9 clear and overcast radiances assimilation, the difference in forecast scores between ASR and CTRL experiments were computed for different variables and regions. Forecast results are computed for 90 days of assimilation experiments.

Figure 17 shows the normalized difference in 500 hPa geopotential and vector wind RMS error in the Northern Hemisphere, Southern Hemisphere and Tropics between the ASR experiment and the control CTRL as a function of forecast range in days. Both experiments have been verified against own analysis. Negative (positive) values indicate a reduction (an increase) in forecast error for the ASR experiment. Error bars highlight the level of significance of the changes based on a 95% confidence level. The reader is referred to Geer *et al.*, (2010) for details on the method used to calculate RMS error and the statistical signifiance of the difference. Averaged over a three month period, 500 hPa height and wind forecast errors are, overall, not statistically significantly different for the ASR experiments and the CTRL.

Some wind forecast improvements in the upper troposphere from the ASR experiment are present in the short range in the Southern Hemisphere at 200 hPa (see figure 18), but the changes are statistically neutral beyond day 3.

## 5.3 Advanced diagnostics

The analysis of the information content of observations and the related contribution in the short-range forecast error are routine activities at ECMWF (Cardinali *et al.*, 2004; Cardinali 2009; Cardinali and Prates, 2011). The DFS and the 24-hour forecast error contribution of all the observing system components has been computed for January 2011, to assess the impact of geostationary CSR and in particular, the impact of SEVIRI clear radiances and combined SEVIRI clear and overcast radiances.

For any data assimilation system, the DFS is used to indicate the self-sensitivity of analysis to different observation types being assimilated. The DFS is the image in observation space of the trace of the derivative

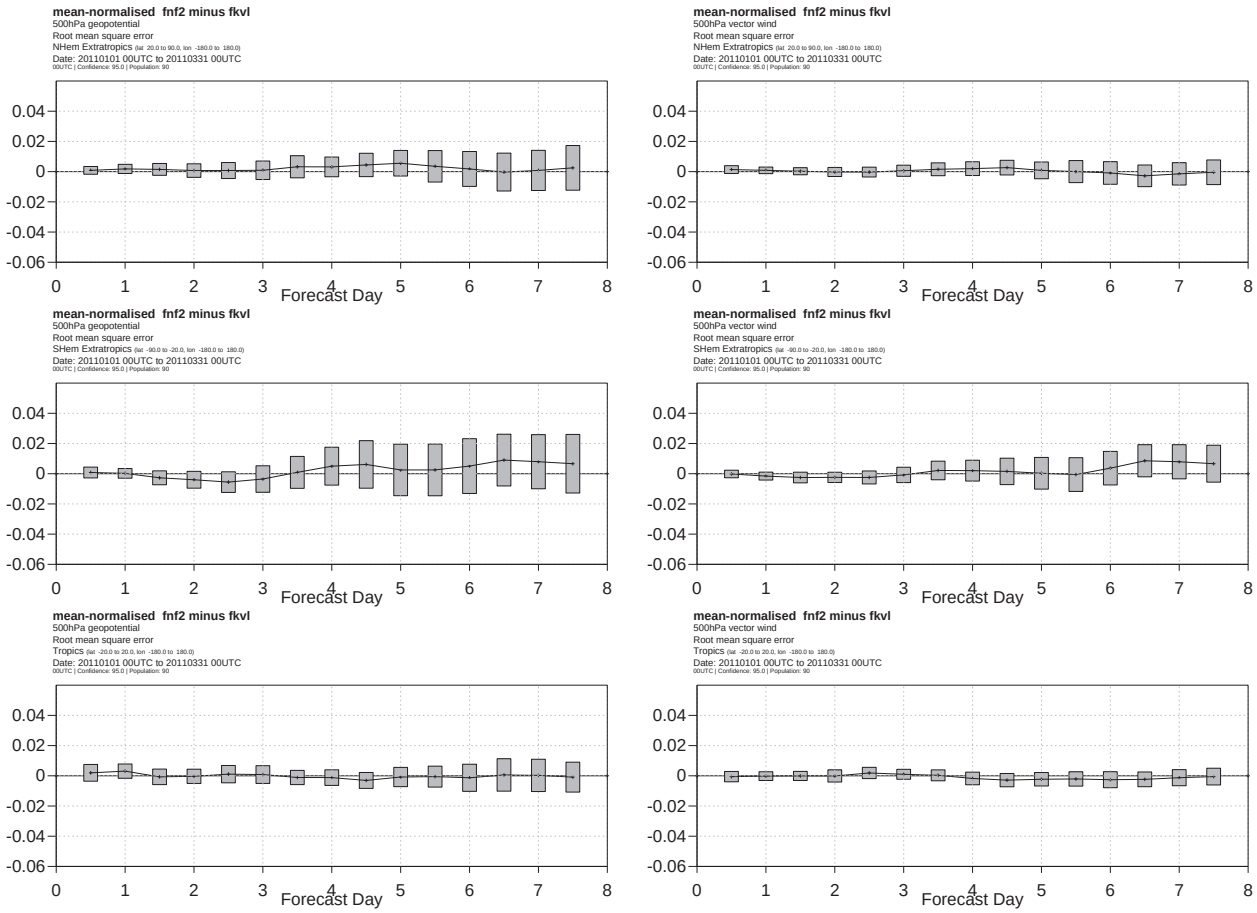


*Figure 17: Normalised difference in the root mean square error (RMS) of the 500 hPa geopotential (left side) and vector wind (right side) between the ASR and the CTRL experiment as verified against own analysis for Northern Hemisphere (top), Southern Hemisphere (middle), Tropics (bottom). Negative values indicate a reduction in the forecast error from using clear and overcast radiances compared to operational CSR. Error bars indicate 95% confidence intervals.*

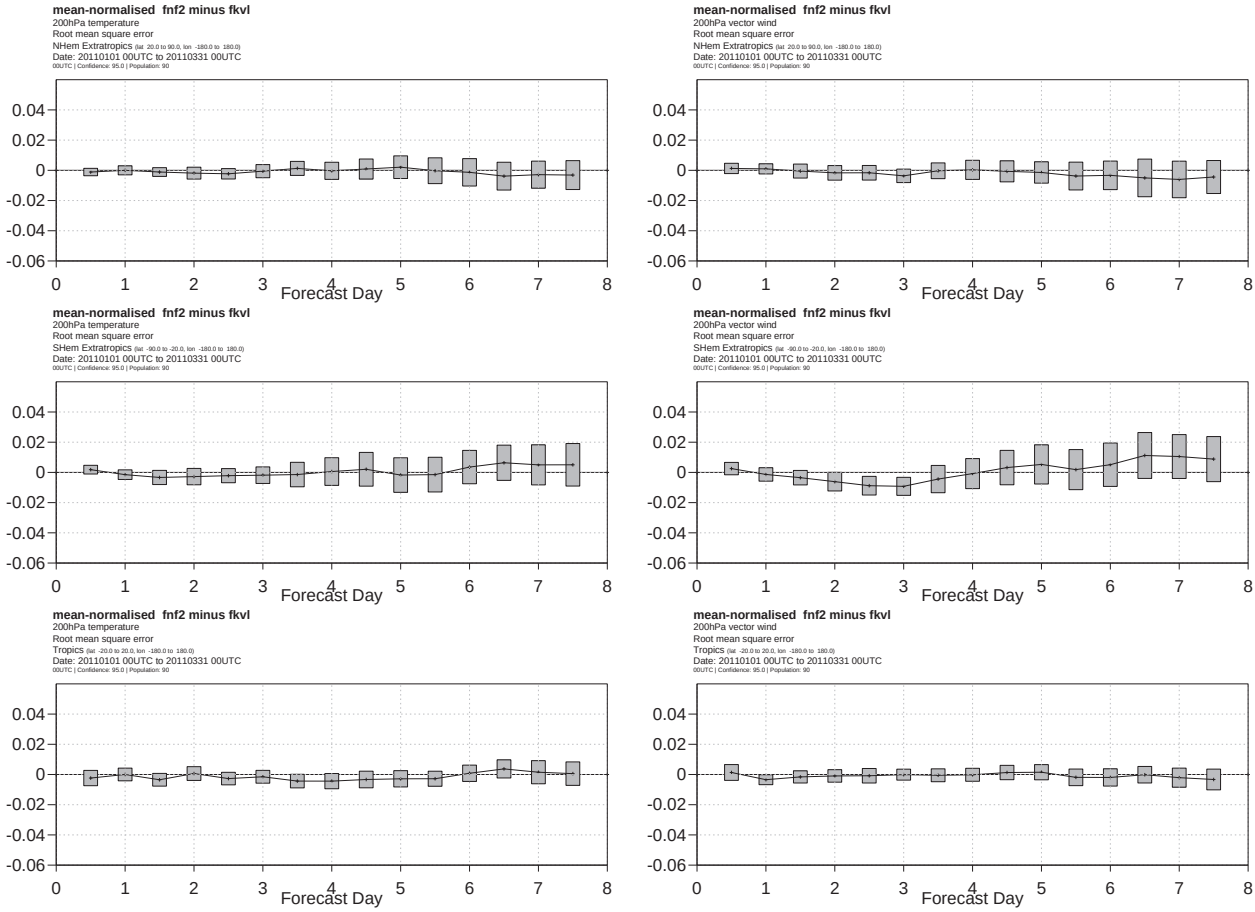


*Figure 18: As Fig. 17 but for the 200 hPa temperature (left side) and vector wind (right side) forecasts.*

of the analysis with respect to observations. The reader is referred to Cardinali *et al.*, (2004) for details on DFS calculations at ECMWF. The DFS is a function of the observation and background covariance matrices, the model itself as a time-spatial propagator and the number of observations. From figure 19 (left side), the largest contribution in the CTRL analysis is provided by AMSU-A (23%), IASI and AIRS (15%), AIREP(8%), GPS-RO(6%) followed by SYNOP, TEMP, HIRS (4%). All other observation types contribute up to 4%. The geostationary radiances and AMVs from five geostationary satellites contribute up to 5%. For any assimilated set of data, the observation influence shown in figure 19 (right side), is defined as the DFS normalized by the number of observations. We note that the observation influence number is in theory comprised between 0 and 1. The occurence of values bigger than one for dribus data is partly due to the self-sensitivity calculation approximation as explained in Cardinali *et al.*, 2004.

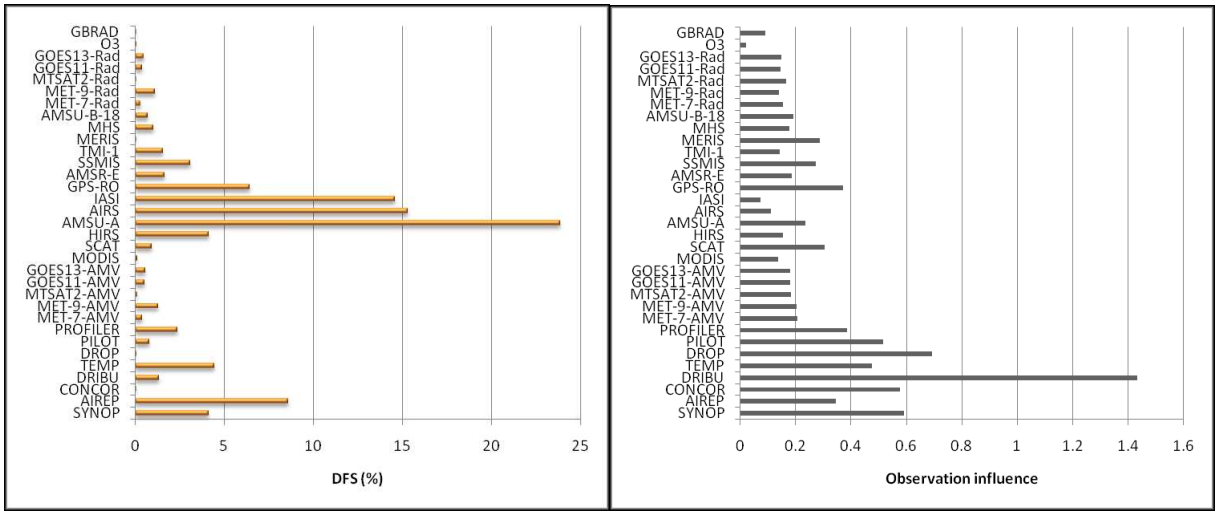


*Figure 19: DFS as percentage (left side) and observation influence (right side) for all observation types assimilated in CTRL experiment in January 2011.*

An observing system experiment (OSE) is a traditional approach to estimate the impact of a specific observing network on a numerical weather prediction system. An OSE is composed of two experiments, both covering the same period. In the first experiment (control), all the observations operationally available are used. In the second experiment, selected datasets are systematically removed from the assimilation procedure to assess the degradation in quality of a model forecast when that observation type is denied (e.g., Kelly et al. 2007). Using such methods the contribution of each observation type is assessed one by one. However, using OSE to assess the observation values of each assimilated observation type to forecast accuracy could be very expensive.

Adjoint-based observation sensitivity procedures have been used to diagnose the impact of all assimilated observations on forecast (Langland and Baker, 2004; Cardinali 2009). The observation contribution to the forecast is evaluated with respect to a scalar function representing the short range forecast error. Using adjoint-based method all observation impacts are produced simultaneously. The impact of any instrument can be computed over the globe or only over an interest area or by instrument channel. Cardinali et al. (2009) and Gelaro and Zhu (2009) have compared adjoint-based impact calculations against results from OSEs. Despite some fundamental differences between adjoint-based and OSE techniques, the general conclusions of these studies were that the two approaches provide unique, and complementary, information. The 24-h forecast error contribution (FEC) presented as a percentage in figure 20 show that the forecast errors decrease for all observation types. When the impact value is negative, this induces a positive influence on the forecast as it reduces the forecast error. Results show that AMSU-A has the largest impact in decreasing the forecast error (23%), followed by AIREP (10%), IASI and AIRS (8%), GPS-RO (6%).

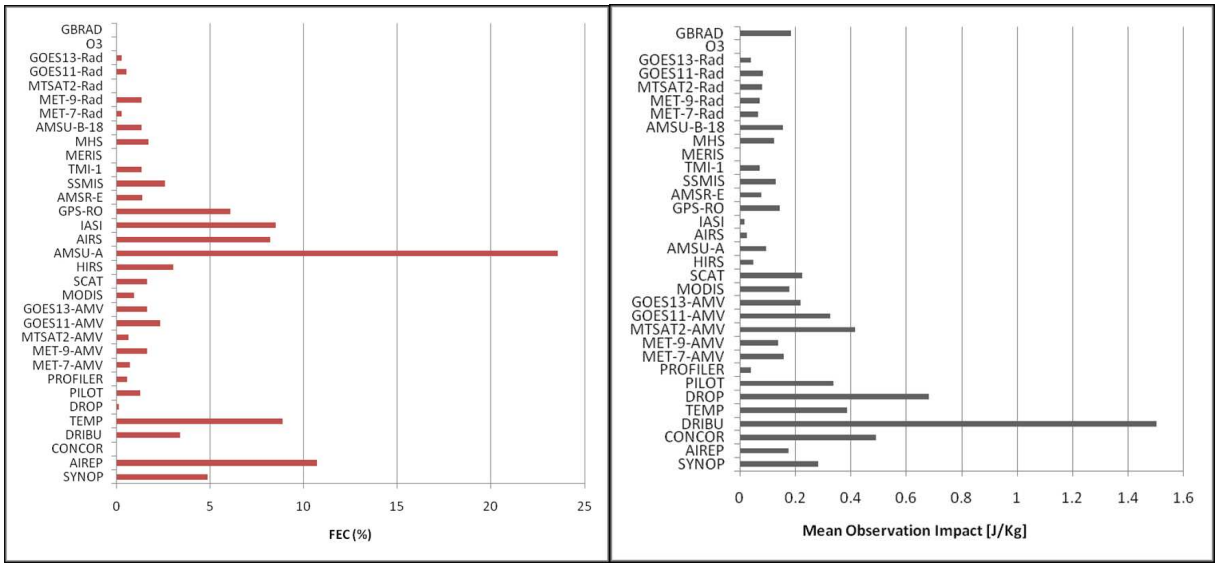


*Figure 20: 24-h forecast error contribution as percentage (left side) and the mean observation impact for all observation types assimilated in CTRL experiment from 1 January to 25 January 2011.*

Figure 21 show the DFS and FEC for the geostationary satellites. Meteosat-9 shows the largest contribution in the analysis among geostationary satellites and this is due to the large numbers of assimilated clear-sky radiances and AMVs. The analysis impact of MTSAT-2 clear-sky radiances is very small particularly, because the MTSAT-2 radiances were blacklisted during the period of this experiment. It is worth mentioning that CSR and AMVs observation influence show quite similar values for all geostationary satellites. AMVs observation influence is larger than CSR observation influence. On the 24-h forecast impact, Meteosat-9 is measured as having the largest contribution to the decrease of forecast error of any geostationary platform, its impact being mainly due to AMVs. The ranking of 24-h forecast error contribution from geostationary satellites is led by Meteosat-9, followed by GOES-11, Meteosat-7 and GOES-13.

In particular, for Meteosat-9, the per channel observation influence and mean observation impact is shown in figure 22 as obtained when the clear-sky radiances (CSR) or the clear radiances combined with the overcast data (ASR) were assimilated. SEVIRI CSR and ASR observation influence in the analysis is very similar with a value of observation influence equal to 0.15 in channel 2 and 0.1 in channel 3, respectively. When comparing the mean observation impact, the largest contribution to the 24-h forecast comes from the combined clear and overcast radiances.

A more detailed diagnostic may be investigated with a robust statistical sample to quantify the individual contributions of the clear and overcast radiances from the ASR. Additionally, forecast error contribution maps will allow us to identify the areas with beneficial or detrimental observation impact. However, the forecast error contribution is only used to diagnose the impact on the short-range forecast, whilst OSEs are more indicated for evaluating the observation forecast impact on the medium and long range.

# 6 Discussion and conclusions

The use of cloudy radiances from satellite instruments in polar or geostationary orbit is still a great challenge for numerical weather prediction. Work is in progress to assimilate such data that should contribute to a more accurate description of the atmospheric state and increased accuracy in numerical weather prediction. This

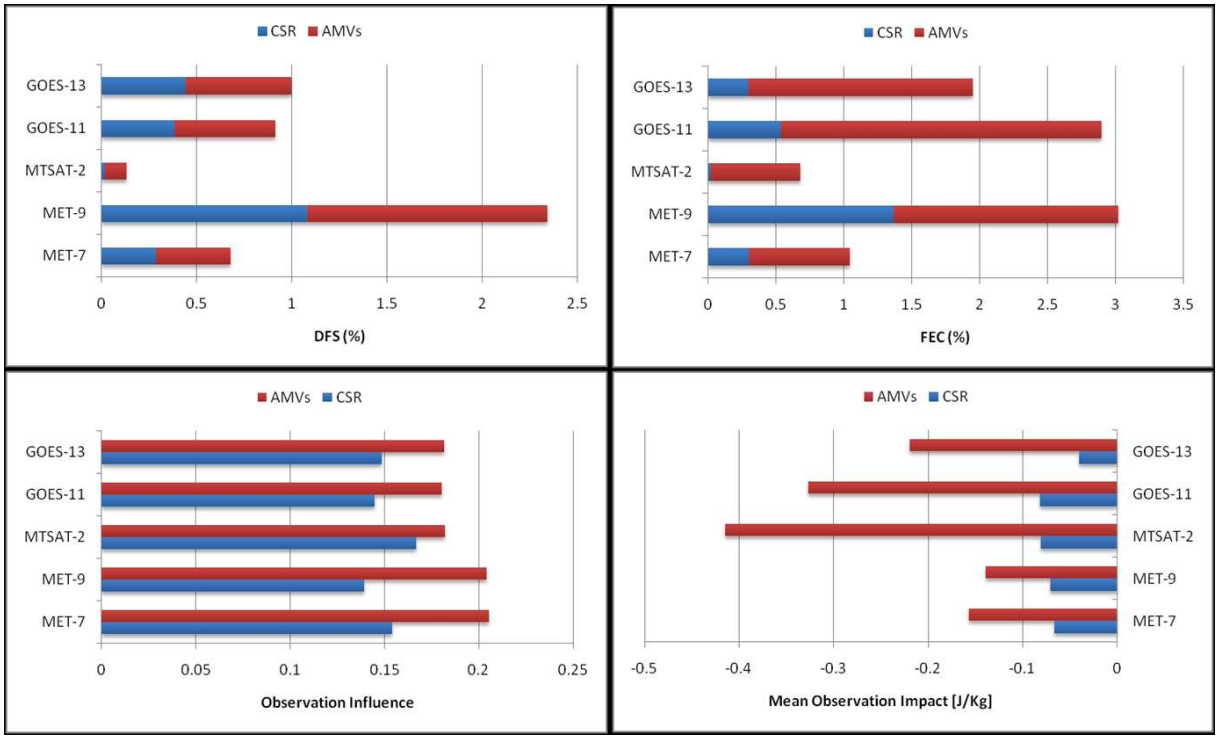


*Figure 21: Top: DFS and 24-h forecast error contribution as percentage for geostationary satellites observations (CSR and AMVs) assimilated from 1 January to 25 January 2011. Bottom: Observation influence and mean observation impact for geostationary satellites observations (CSR and AMVs) assimilated from 1 January to 25 January 2011.*

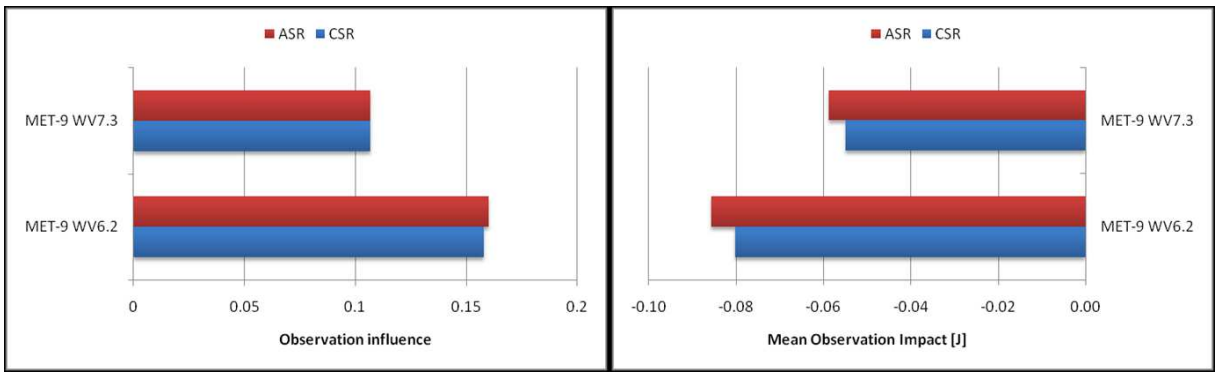


*Figure 22: 24 h forecast error contribution as percentage for geostationary observations assimilated from 1 January to 25 January 2011.*

report documents the introduction of cloud-affected radiances from the Meteosat-9 SEVIRI instrument into the ECMWF Integrated Forecasting System, starting with the assimilation of cloud-affected radiances for restricted conditions such as overcast scenes. The main findings of this work are summarized in the executive summary at the beginning of the report. Here we briefly summarise them.

In the first part of the work, the ECMWF 4D-Var analysis system has been successfully extended to directly assimilate cloud-affected geostationary radiances in overcast conditions from Meteosat-9. We have chosen to use the observation depleted baseline system as reference first, to assess the individual impact of overcast SEVIRI data on ECMWF 4D-Var analysis. The assimilation of fully overcast infrared radiances have been shown to systematically affect temperature, humidity and winds analysis increments in area of overcast cloud regimes showing a very good correspondence between the altitude where the changes occur and the diagnosed height of the overcast cloud. One of the main results was that overcast geostationary images from SEVIRI have a small positive impact on improving the wind analysis scores. By relaxing the overcast definition to scenes with an estimated effective cloud fraction greater than 0.99, the number of assimilated cloud-affected SEVIRI data is increasing and this enhances the impacts that have been demonstrated on wind analysis.

In the second part of this work the focus was to investigate the relative-humidity and wind analysis impact of each of the following observations types from Meteosat-9 SEVIRI: clear-sky radiances, overcast and AMVs. The geostationary overcast radiances in four channels were used only over sea while clear-sky radiances from the 6.2$\mu$m and 7.3$\mu$m water-vapour channels were used also over land. The analysis impact of each of those observation types was expressed in terms of the root-mean-square of humidity and wind speed analysis difference with respect to the baseline assimilation and was shown as vertical profiles on pressure levels between 1000 and 1 hPa inside Meteosat-9 disc area. The WV CSR have a positive impact on wind analysis and the maximum was found at 300 hPa and 500 hPa. For the cloudy AMVs, the maximum impact on wind analysis was obtained at 250 hPa and 850 hPa. The vertical profiles of winds speed from overcast SEVIRI and AMVs assimilated over sea have shown a main peak located at 250-300 hPa. The impact of AMVs is larger as the number of completely overcast SEVIRI scenes is reduced comparatively with the number of cloudy AMVs. Further, assimilated overcast radiances on-top of already assimilated clear-sky SEVIRI radiances have a positive impact on wind analysis through the troposphere with a better performance than clear-sky radiances over the Southern Hemisphere. This result demonstrate that additional dynamical information was extracted from the assimilated cloud-affected SEVIRI radiances. The last part of this work focussed on the assessment of the impact of cloud-affected SEVIRI radiances in the full system. While results for the current implementation of the scheme already used for hyperspectral sounders are encouraging, some issues remain to be addressed to be able to extend the geostationary infrared situations to non-overcast situations. At the present time, it was important to examine the capabilities of extracting wind information from the assimilation of geostationary data, in order to guide preparations for the next generation of hyperspectral infrared sounders on geostationary orbit.

# 7 Acknowledgements

Cristina Lupu's work at ECMWF was funded through a EUMETSAT research fellowship. Anne Fouilloux, Alan Geer, Niels Bormann and Carla Cardinali are thanked for their help in this work. The authors thank to Stephen English and Jean-Noël Thépaut for their internal review of the manuscript.

## References

Bauer P., T. Auligné, W. Bell, A. Geer, V. Guidard, S. Heilliette, M. Kazumori, M.-J. Kim, E.H.-C. Liu, A.P. McNally, B. Macpherson, K. Okamoto, R. Renshaw, L.-P. Riishjgaard, 2011: Satellite cloud and precipitation assimilation at operational NWP centres, *Q. J. R. Meteorol. Soc.*, **137**, 1934-1951.

Cardinali C., S. Pezzulli , E. Andersson, 2004: Influence matrix diagnostics of a data assimilation system. *Q. J. R. Meteorol. Soc.*, **130**, 2767-2786.

Cardinali C., 2009: Monitoring the observation impact on the short-range forecast. *Q. J. R. Meteorol. Soc.*, **135**, 239-250.

Cardinali C, F. Prates, 2011: Performance measurement with advanced diagnostic tools of all-sky microwave imager radiances in 4D-Var. *Q.J. R. Meteorol. Soc.* **137**, 2038-2046.

Chevallier, F., P. Lopez, A. Tompkins, M. Janisková, E. Moreau, 2004: The capability of 4D-Var systems to assimilate cloud-affected satellite infrared radiances. *Q. J. R. Meteorol. Soc.*, **130**, 917-932.

Dee, D. P., 2004: Variational bias correction of radiance data in the ECMWF system. Proceedings of the ECMWF workshop on assimilation of high spectral resolution sounders in NWP, 28 June-1 July 2004. Reading, UK.

Eyre, J. R., and W. P. Menzel, 1989: Retrieval of cloud parameters from satellite sounder data: A simulation study. *J. Appl. Meteor.*, **28**, 267-275.

Geer, A. J., P. Bauer, and P. Lopez, 2010: Direct 4D-Var assimilation of all-sky radiances. Part II: Assessment. *Q. J. R. Meteorol. Soc.*, **136**, 1886-1905.

Gelaro, R., and Y. Zhu, 2009: Examination of observation impacts derived from observing system experiments (OSEs) and adjoint models. *Tellus*, **61A**, 179-193.

Heilliette, S., and L. Garand. 2007: A practical approach for the assimilation of cloudy infrared radiances and its evaluation using AIRS simulated observations.*Atmosphere-Ocean*, **45(4)**, 211-225.

Kelly, G., J-N. Thépaut, R. Buizza, and C. Cardinali, 2007: The value of observations. I: Data denial experiments for the Atlantic and the Pacific. *Quart. J. Roy. Meteor. Soc.*, **133**, 1803-1815.

Köpken, C., G. Kelly and J-N. Thépaut, 2004: Assimilation of Meteosat radiance data within the 4D-Var system at ECMWF: Data quality monitoring, bias correction and single-cycle experiments. *Q. J. R. Meteorol. Soc.*, **130**, 2293-2313.

Langland, R. H., and N. L. Baker, 2004: Estimation of observation impact using the NRL atmospheric variational data assimilation adjoint system. *Tellus*, **56A**, 189-201.

Lupu, C., and A. McNally, 2011a: Assimilation of radiance products from geostationary satellites: 1-year report. EUMETSAT/ECMWF Fellowship Programme Research Reports No.21, 27 pp.

Lupu, C., and A. McNally, 2011b: Assimilation experiments with the cloud-affected geostationary observations at ECMWF, Proceedings 2011 EUMETSAT Meteorological Satellite Conference, 5-9 September 2011, Oslo, Norway.

Matricardi, M., F. Chevallier, G. Kelly, J.-N. Thépaut, 2004: An improved general fast radiative transfer model for the assimilation of radiance observations. *Q. J. Roy. Meteorol. Soc.*, **130**, 153-173.

McNally, A., 2002: A note on the occurrence of cloud in meteorologically sensitive areas and the implications for advanced infrared sounders. *Q. J. R. Meteorol. Soc.*, **128**, 2551-2556.

McNally, A., 2009: The direct assimilation of cloud-affected satellite infrared radiances in the ECMWF 4D-Var. *Q. J. R. Meteorol. Soc.*, **135**, 1214-1229.

Munro, R., C. Köpken, G. Kelly, J-N. Thépaut and R. Saunders, 2004: Assimilation of Meteosat radiance data within the 4D-Var system at ECMWF: Assimilation experiments and forecast impact. *Q. J. R. Meteorol. Soc.*, **130**, 2277-2292.

Okamoto, K., 2012: Assimilation of overcast cloudy infrared radiances of the geostationary MTSAT-1R imager. (submitted to *Q. J. R. Meteorol. Soc.*)

Pangaud, T., N. Fourrie, V. Guidard, M. Dahoui, F. Rabier, 2009: Assimilation of AIRS Radiances Affected by Mid- to Low-Level Clouds. *Mon. Wea. Rev.*, **137**, 4276-4292.

Pavelin, E. G., S. J. English, and J. R. Eyre, J. R. 2008, The assimilation of cloud-affected infrared satellite radiances for numerical weather prediction. *Q. J. R. Meteorol. Soc.*, **134**, 737-749.

Peubey, C., and A. P. McNally, 2009: Characterization of the impact of geostationary clear sky radiances on wind analyses in a 4D-Var context. *Q. J. R. Meteorol. Soc.*, **135**, 1863-1876.

Schmetz, J, P. Pili, S. Tjemkes, D. Just, J. Kerkmann, S. Rota, A. Ratier, 2002: An Introduction to Meteosat Second Generation (MSG). *Bull. Amer. Meteor. Soc.*, **83**, 977-992.

Stengel, M., P. Undén, M. Lindskog, P. Dahlgren, N. Gustafsson, R. Bennartz, 2009: Assimilation of SEVIRI infrared radiances with HIRLAM 4D-Var. *Q. J. R. Meteorol. Soc.*, **135**, 2100-2109.

Stengel, M., M. Lindskog, P. Undén, N. Gustafsson, R. Bennartz, 2010: An extended observation operator in HIRLAM 4D-VAR for the assimilation of cloud-affected satellite radiances. *Q. J. R. Meteorol. Soc.*, **136**, 1064-1074.

Szyndel, M. D. E., G. Kelly, J.-N. Thépaut, 2005: Evaluation of potential benefit of assimilation of SEVIRI water vapour radiance data from Meteosat-8 into global numerical weather prediction analyses. *Atmos. Sci. Let.*, **6**, 105-111.

## APPENDIX I: Validation experiments using SEVIRI clear sky radiances

As the ASR extend the information already available in the operational CSR product, validation of clear radiances from the new ASR was accomplished through comparisons to the operational CSR product.

Experiments have been run in the global 4D-Var configuration with 12-hour assimilation window for winter period (1 January 2011 - 1 March 2011) and were based on a lower than operational horizontal resolution (T511 rather than T1279) to save computer resources. Initial conditions came from the operational analyses for 12Z on 31st December 2010. Only one medium-range forecast has been run per day as opposed to two forecasts in the operational configuration. The experiments carried out were therefore:

- Control experiment CTRL (*fkvl*) used all available conventional and satellite data, including WV clear-sky radiances from Meteosat-9 from EUMETSAT CSR product.
- Experiment EXP1 (*fmr0*) is identical with the control experiment except that WV clear SEVIRI radiances from the new ASR product are assimilated in the place of SEVIRI WV clear radiances from CSR product.
- Experiment EXP2 (*fms1*) has been designed to test the cloudy assimilation scheme with SEVIRI ASR clear and overcast observations. The experiment EXP2 uses the same selection criteria for the assimilation of WV clear SEVIRI radiances as the previous experiment EXP1 and exclude all scenes identified as overcast in the cloud parameters estimation process. The purpose of this experiment was to technically check the cloudy assimilation approach code changes and to validate that the performance of the assimilation system remain unchanged when only the clear SEVIRI dataset is assimilated.

Similar data selection and blacklist change criteria are applied in both CTRL and EXP1 experiments, except that no basics check on satellite zenith angles are done prior to the insertion into IFS. An examination of ASR BUFR file prior to the assimilation shows that for WV channel at 6.2$\mu$m, the sum of pixels flagged as clear-sky and of pixels with low-level clouds is the equivalent percentage of clear pixels provided with the CSR product. Additionally, SEVIRI observations from the new ASR product are rejected if the total percentage of pixels flagged as cloudy and clear-sky in a segment is less than 100%.

The overall characteristics of the first guess or analysis departures for clear SEVIRI radiances are unchanged when the new ASR product is used (not shown). For other assimilated observations, there is no significant impact on the departure statistics, suggesting no significant change to the quality of the first guess or the analysis.

Forecast results are computed for different variables and regions for 60 days of assimilation experiments. The forecast scores are calculated as the normalised difference in root mean square errors between the EXP1 and CTRL and EXP2 and CTRL, respectively. Each experiment's own analyses is used as the reference.

Figures 23 show normalised difference in the root mean squared forecast error (RMS) between the EXP1 experiment and the CTRL for the 00Z forecast of the 500 hPa geopotential and temperature, for 1 January 2011 to 1 March 2011. Positive differences in RMS indicate a degradation in the EXP1 experiment compared to the control and negative differences show an improvement. Error bars indicate the 95% confidence range for a significant difference between experiment and control. There is no significant change to geopotential forecasts between forecast day 1 and 8.

The forecast impact of the EXP_CSR versus the CTRL is mostly neutral (see figure 24 for the forecast of the 500 hPa geopotential and temperature).

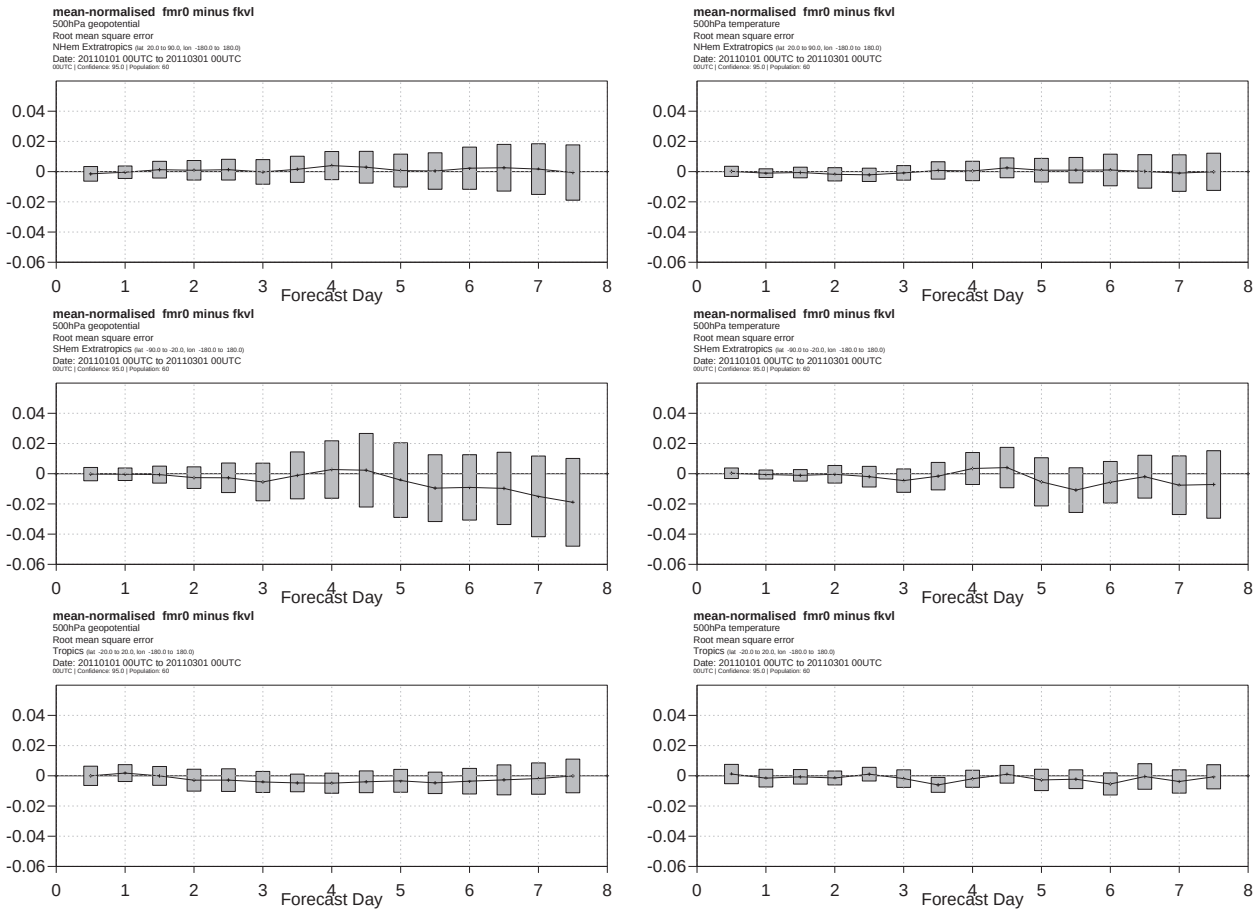


*Figure 23: Normalised difference in the root mean square error (RMS) of the 500 hPa geopotential (left side) and temperature (right side) between the EXP1 and the CTRL experiments as verified against own analysis for Northern Hemisphere (top), Southern Hemisphere (middle), Tropics (bottom). Negative values indicate a reduction in the forecast error from using clear radiances from ASR compared to operational CSR. Error bars indicate 95% confidence intervals.*

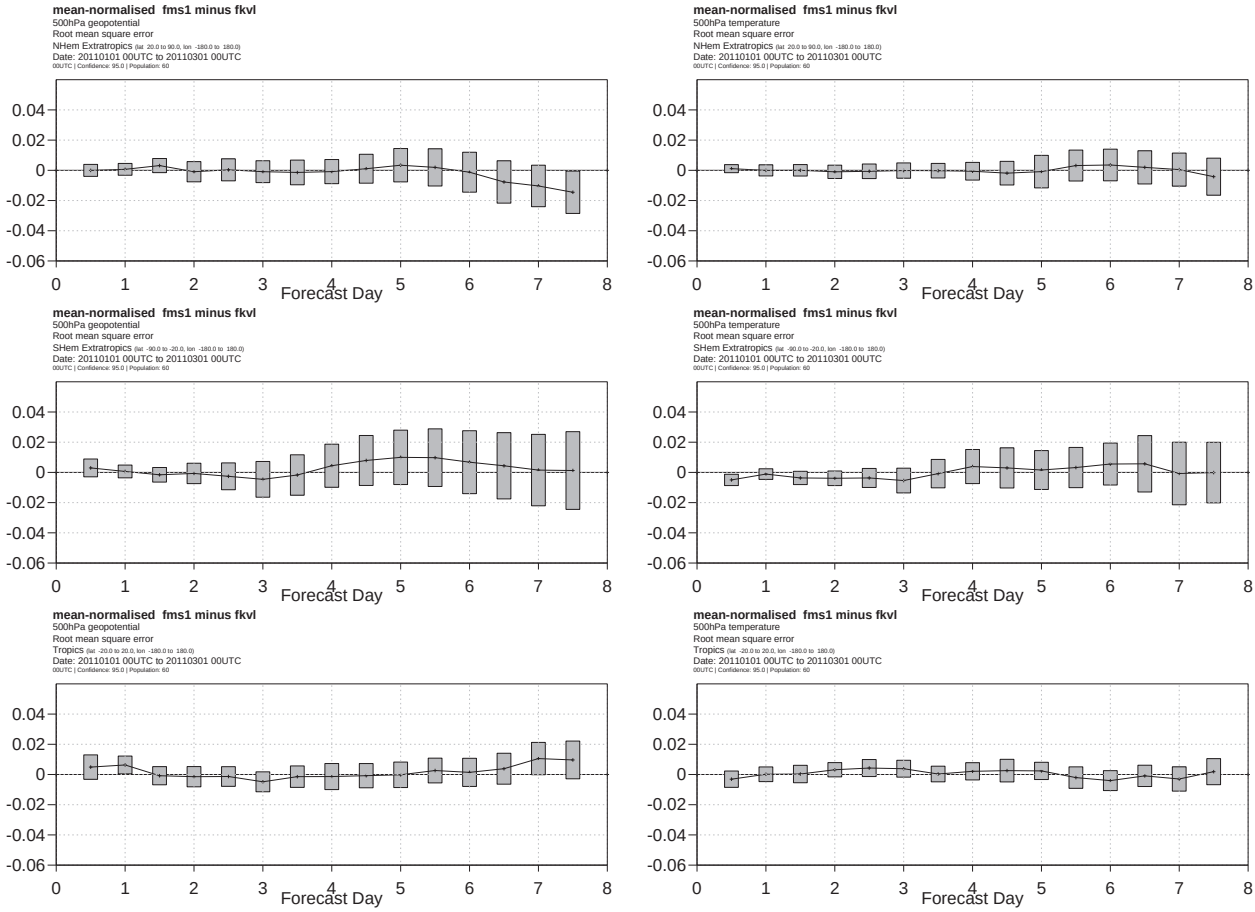


*Figure 24: As Fig. 23 but for the EXP2 compared to the CTRL experiment*

## APPENDIX II: Accronyms and abbreviations

| | |
|---|---|
| 4D-Var | Four-dimensional variational data assimilation |
| AIRS | Atmospheric InfraRed Sounder |
| AMVs | Atmospheric Motion Vectors |
| CSR | Clear Sky Radiances |
| ASR | All Sky Radiances |
| DFS | Degrees of Freedom for Signal |
| ECMWF | European Centre for Medium Range Weather Forecast |
| EUMETSAT | European Organisation for the Exploitation of Meteorological Satellites |
| FEC | Forecast Error Contribution |
| HIRS | High Resolution Infrared Radiation Sounder |
| HIRLAM | HIgh Resolution Limited Area Model |
| IASI | Infrared Atmospheric Sounding Interferometer |
| IFS | Integrated Forecasting System |
| IR | Infrared |
| NWP | Numerical Weather Prediction |
| OSE | Observing System Experiment |
| RMS | Root Mean Square forecast error |
| RTTOV | Radiative Transfer for TOV |
| SEVIRI | Spinning Enhanced Visible and Infrared Imager |
| WV | Water vapour |